The International Linear Collider

Leif Jönsson
Lund University

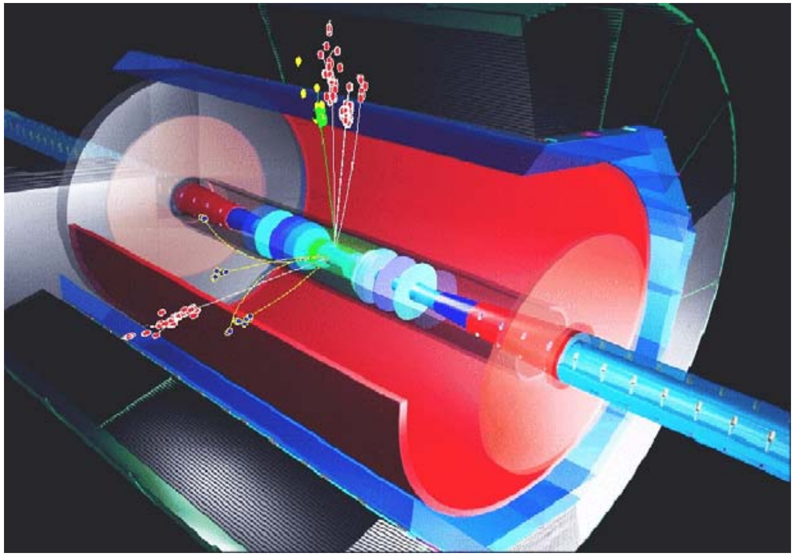

Introduction
The physics case; some examples
The accelerator
The detector
- the vertex detector
- the TPC
- the calorimeter

Introduction

1995: 1st DESY/ECFA Workshop series on future e^+e^--colliders.

Uppsala, April 25-26, 1996: a symposium on Future Electron Accelerators and Free Electron Lasers

Lund, June 28-30, 1998 a workshop meeting in the series '2nd ECFA/DESY Study on Physics and Detectors'

2004: Important decisions:

Scientists from throughout the worldwide particle physics community have endorsed an electron-positron linear collider as the next high-energy particle accelerator.

The 12-member International Technology Recommendation Panel, chaired by Barry Barish of the California Institute of Technology, recommended that the world particle physics community adopt superconducting accelerating structures that operate at 2 Kelvin, rather than "X-band" accelerating structures operating at room temperature, as the technology choice for the internationally-federated design of a new electron-positron linear collider to operate at an energy between 0.5 and 1 TeV.

"A linear collider is the logical next step to complement the discoveries that will be made at the LHC," Aymar said. "The technology choice is an important step in the path towards an efficient development of the international TeV linear collider design, in which CERN will participate."

2004: EuroTeV, 2006: EURODET, 2009: DevDet?

Physics

The physics agenda for the ILC

- Higgs
  - The Standard Model Higgs
  - SUSY Higgs
- Non-SUSY extensions of SM
- SUSY
  - Minimal Supersymmetric Standard Model (MSSM)
  - The Minimal Supergravity model (mSUGRA)
  - Gauge-Mediated SUSY Breaking (GSMB)
  - Anomaly-Mediated SUSY Breaking (AMSB)
- Alternative theories
  - Extra Dimensions
  - Strong electroweak symmetry breaking
  - Compositness
- Precision measurements
  - Electroweak Gauge bosons
  - Extended Gauge theories
  - Top quark physics
  - Quantum Chromodynamics

- J.A. Aguilar-Saavedra et al., hep-ph/0106315
- T. Abe et al., hep-ex/0106055
- K. Abe et al., hep-ph/0109166
- G. Weiglein et al., hep-ph/0410364

Very much the same as LHC
Why do we need the ILC?
Key words:

- Complementarity
- Precision

General remarks

LHC:

\+ Large mass range for direct searches (6-7 TeV for singly produced particles, 2-3 TeV for pair produced)

\+ High luminosity (10^{34})

\+ Access to coloured particles (squarks and gluinos)

\- Huge QCD-background (irreducable)

\- High collision frequency (25 MHz→pile-up of events)

ILC:

\+ Cleaner experimental environment

\+ Initial state well defined (important for precision measurements)

\+ Precision measurements give indirect sensitivity to new physics beyond LHC (typically 10 TeV)

\+ High luminosity ($5\cdot10^{34}$)

\+ Favourable signal/background situation (reducable background)

\+ Low collision frequency (can run 'triggerless')

\- Beamstrahlung background

Higgs

LHC: Direct measurement of heavier Higgs (provided the bgr is manageable)
If $h \to \gamma\gamma$ accesible then $\Delta m_h \approx 200$ MeV
Other decay channels give Δm_h much worse

ILC: Precise measurements on light Higgs bosons

Higgs strahlung: $e^+e^- \to ZH$

- Clear experimental signal
- $\Delta M_H = 50$ MeV

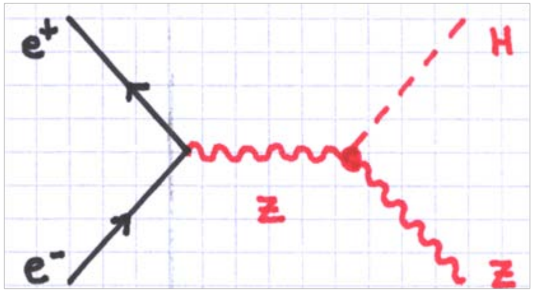

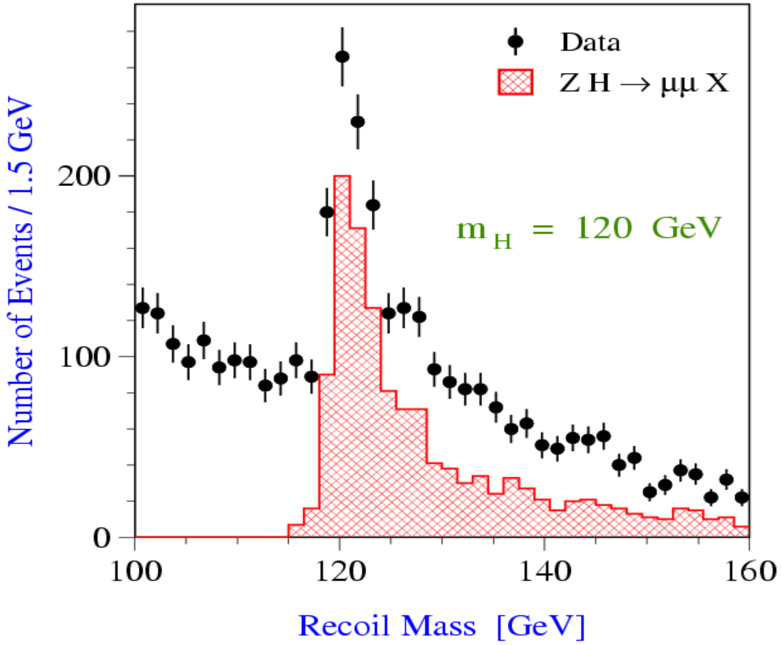

Theory: The prediction of m_h is sensitive to radiative corrections from top
⇒ needs $\Delta m_t < 0.1$ GeV from ILC

Higgs couplings

- Important to measure the couplings to as many particles as possible.
- Some couplings can be determined independently from different observables whereas others are partially correlated

⇒ Extract Higgs couplings from a global fit to the measured observables (σ_{HZ}, $\sigma_{H\nu\nu}$, BR($H^0 \rightarrow WW$), BR($H^0 \rightarrow \gamma\gamma$), BR($H^0 \rightarrow bb$), BR($H^0 \rightarrow \tau\tau$), BR($H^0 \rightarrow gg$), BR($H^0 \rightarrow cc$), σ_{ttH})

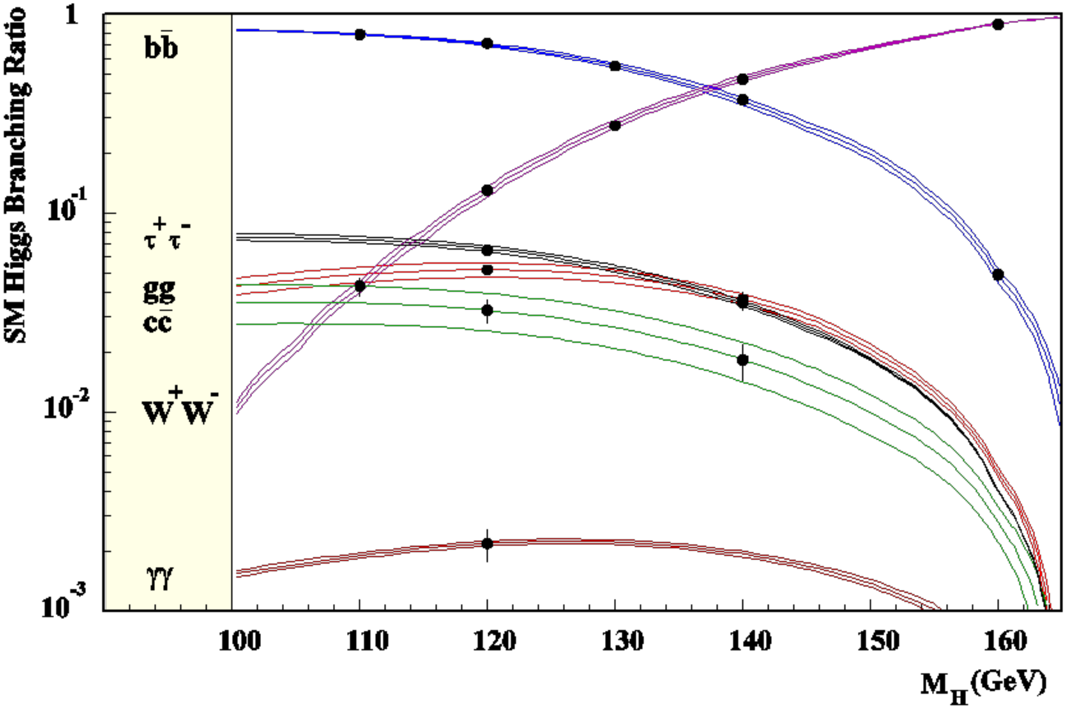

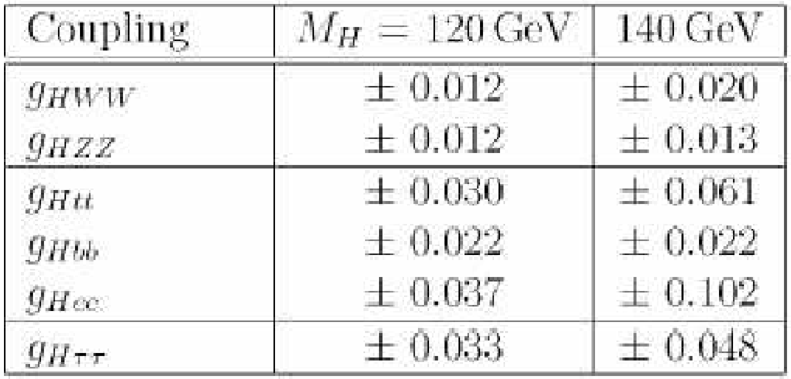

Coupling	$M_H = 120$ GeV	140 GeV
g_{HWW}	$\pm\, 0.012$	$\pm\, 0.020$
g_{HZZ}	$\pm\, 0.012$	$\pm\, 0.013$
g_{Htt}	$\pm\, 0.030$	$\pm\, 0.061$
g_{Hbb}	$\pm\, 0.022$	$\pm\, 0.022$
g_{Hcc}	$\pm\, 0.037$	$\pm\, 0.102$
$g_{H\tau\tau}$	$\pm\, 0.033$	$\pm\, 0.048$

Accuracy $\delta(X)/X$ in the measurements of Higgs couplings

The Yukawa coupling

- Since the top quark decays much faster than the typical time for top hadron formation, it provides a clean source of fundamental information. Accurate measurements of m_t, couplings (to gauge bosons and Higgs) and BR's probe possible deviations to the SM.

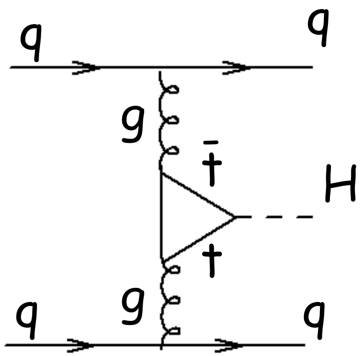

LHC ~ 10-30%

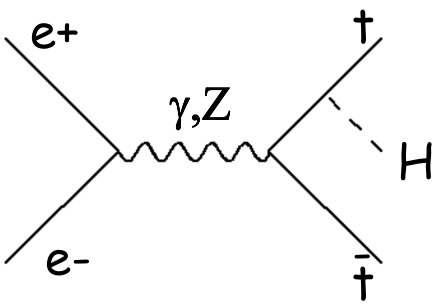

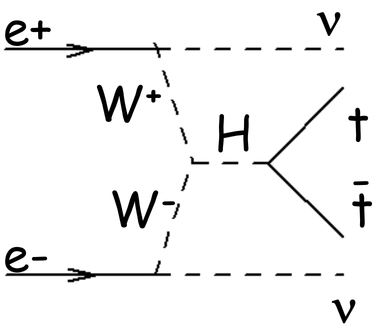

- ILC: the Yukawa coupling htt can only be measured with limited precision at $\sqrt{s}$ = 500 GeV for a light Higgs boson (few events). At $\sqrt{s}$ = 800 GeV ILC will do a good job (4-5 % accuracy)
- LHC: provides the $t\bar{t}h$ production cross section ~ $g_{ttH} \times BR(h \rightarrow b\bar{b}$ or $h \rightarrow W^+W^-)$
- ILC: provides precision measurements of BR's

  Combine LHC and ILC ⇒ Precision measurement

Higgs self-coupling

- The maybe most important measurement, after the Higgs has been established, is the Higgs-boson self coupling, which is needed for the reconstruction of the Higgs potential. Directly probed by multi-Higgs production.

$V(\eta_H) = 1/2 m_H^2 \eta_H^2 + \lambda v \eta_H^3 + 1/4 \lambda \eta_H^4$

η_H is the physical Higgs field
λ is the Higgs boson couplings

LHC:

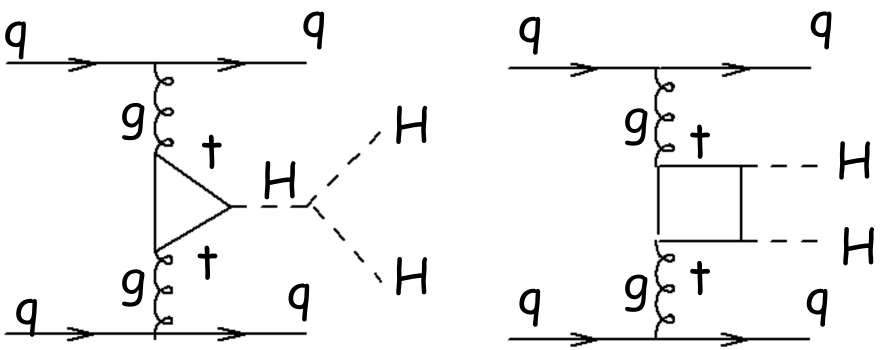

ILC:

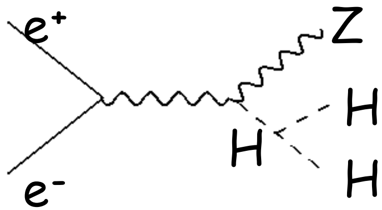

$m_H < 160$ GeV

LHC: Higgs pair production dominated by gluon fusion
Serious background problems ⇒ low sensitivity

ILC: $e^+e^- \rightarrow ZHH \Rightarrow$ precision on $\lambda \sim 23\%$ for a lumi of 1 ab^{-1} $\sqrt{s} = 500$ GeV

$m_H > 160$ GeV

LHC: Higgs decay into W-pairs, SLHC gives a 20-30% measurement of λ
However, to control systematic uncertainties associated with Higgs BR's and the top Yukawa coupling, information from the ILC is needed.

Sparticle mass spectrum

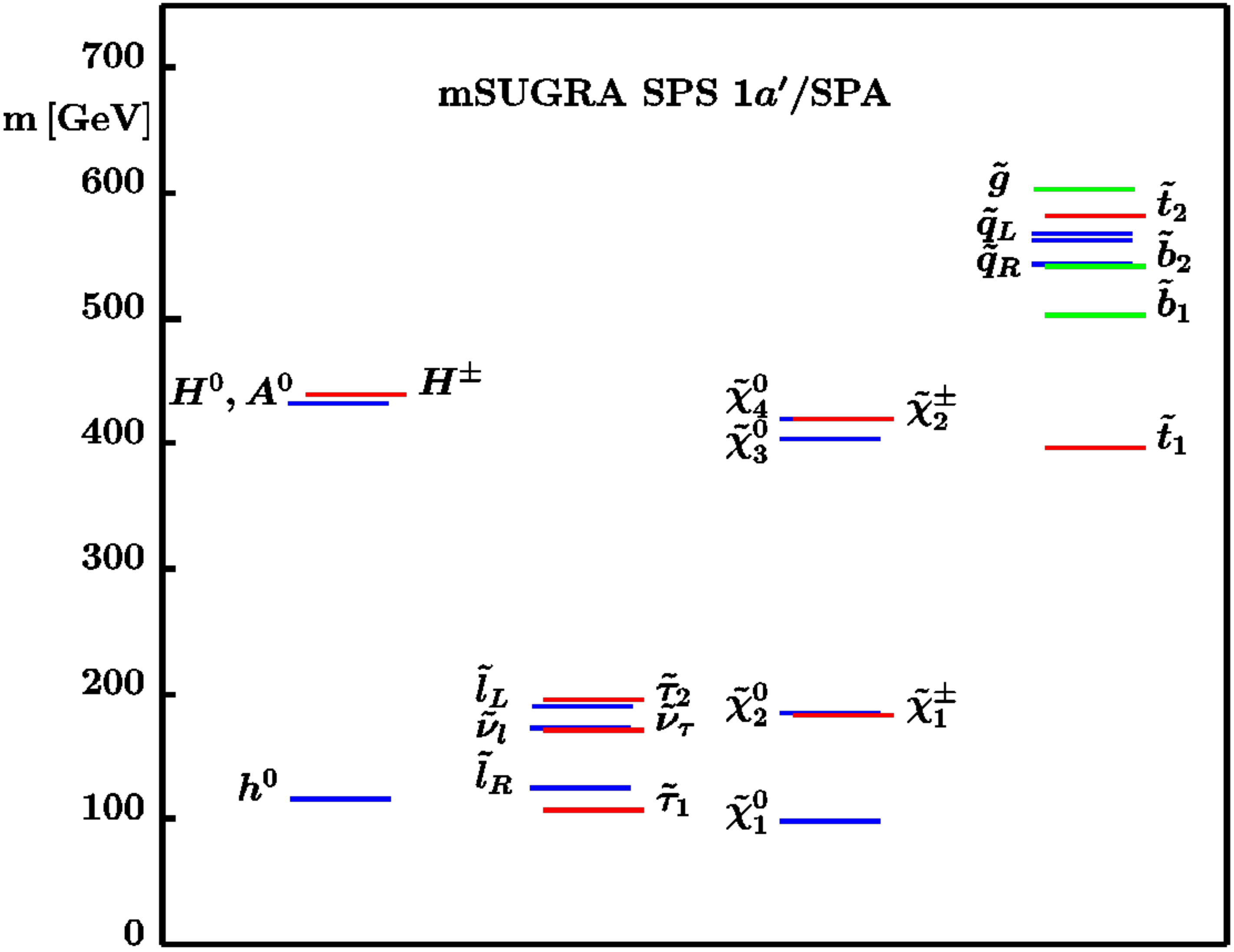

Mass determination

Gluino decay:

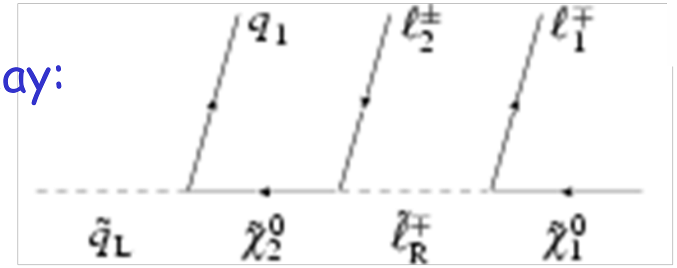

$$\tilde q \to q\,\tilde\chi_2^0 \to q\,(\tilde\ell\ell) \to q\,(\ell\ell)\,\tilde\chi_1^0$$

LHC: Edge effects in cascade decay
⇒ mass-differences
⇒ strong correlation between masses

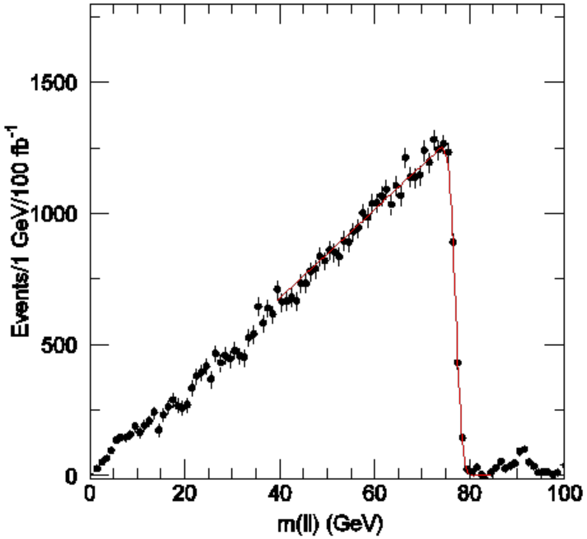

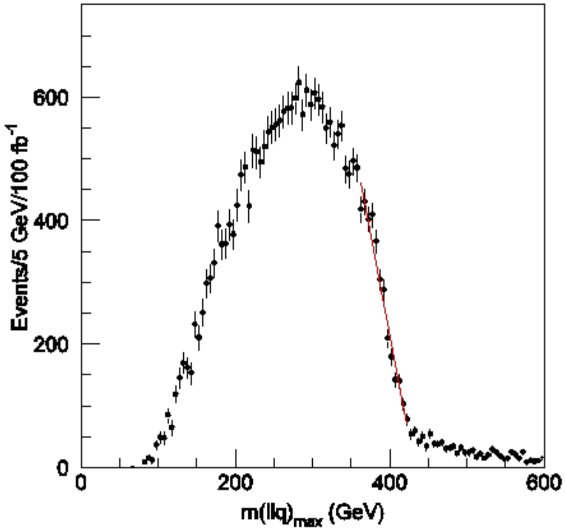

$m^2(ll)=\{(m^2(\tilde\chi_2^0)-m^2(\tilde l_R))(m^2(\tilde l_R)-m^2(\tilde\chi_1^0))\}/m^2(\tilde l_R)$

$m^2(qll)=\{(m^2(\tilde q_L)-m^2(\tilde\chi_2^0))(m^2(\tilde\chi_2^0)-m^2(\tilde\chi_1^0)\}/m^2(\tilde\chi_2^0)$

Mass determination

a) Edge effects: $\tilde{\mu}_R \rightarrow \mu + \tilde{\chi}_1^0$

$$m_{\tilde{\ell}} = \sqrt{s}\sqrt{E_+E_-}/(E_+ + E_-)$$

$$m_{\tilde{\chi}_1^0} = m_{\tilde{\ell}}\sqrt{1 - 2(E_+ + E_-)/\sqrt{s}}$$

precision on χ_1^0 increased by $\sim 10^2$

where E_+ and E_- are the end point energies

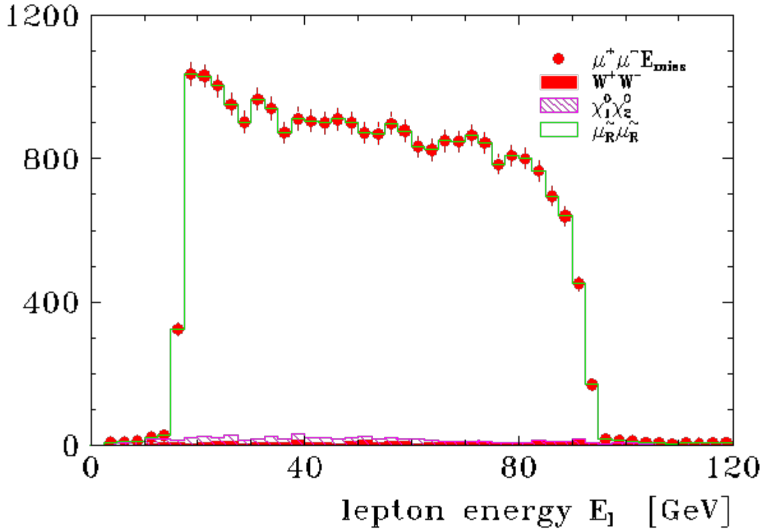

b) threshold excitations:

$$e^+e^- \rightarrow \tilde{\mu}_R^+ + \tilde{\mu}_R^- \rightarrow \mu^+\mu^- + E_{miss}$$

P-wave: slow β^3 rise

$$e^-e^- \rightarrow \tilde{e}_R^- + \tilde{e}_R^- \rightarrow e^-e^- + E_{miss}$$

S-wave: fast β rise

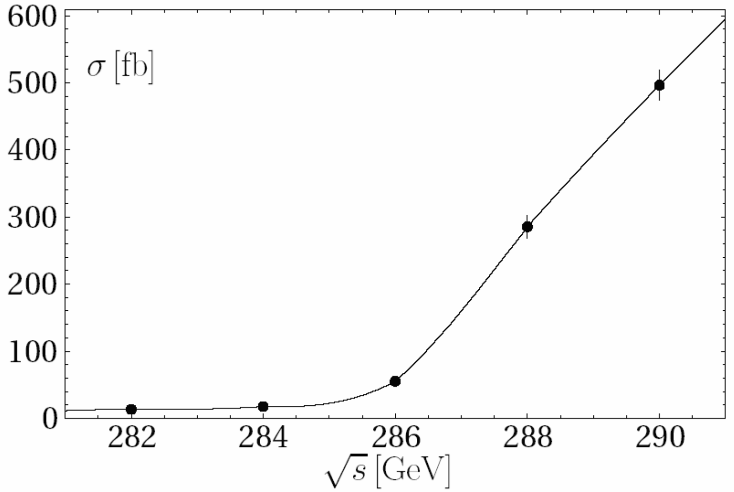

Supersymmetry

SPS1a input parameters: $M_{1/2}$ = 250 GeV, M_0 = 100 GeV, A_0 = -100 GeV, sign(μ) = +, tanβ = 10

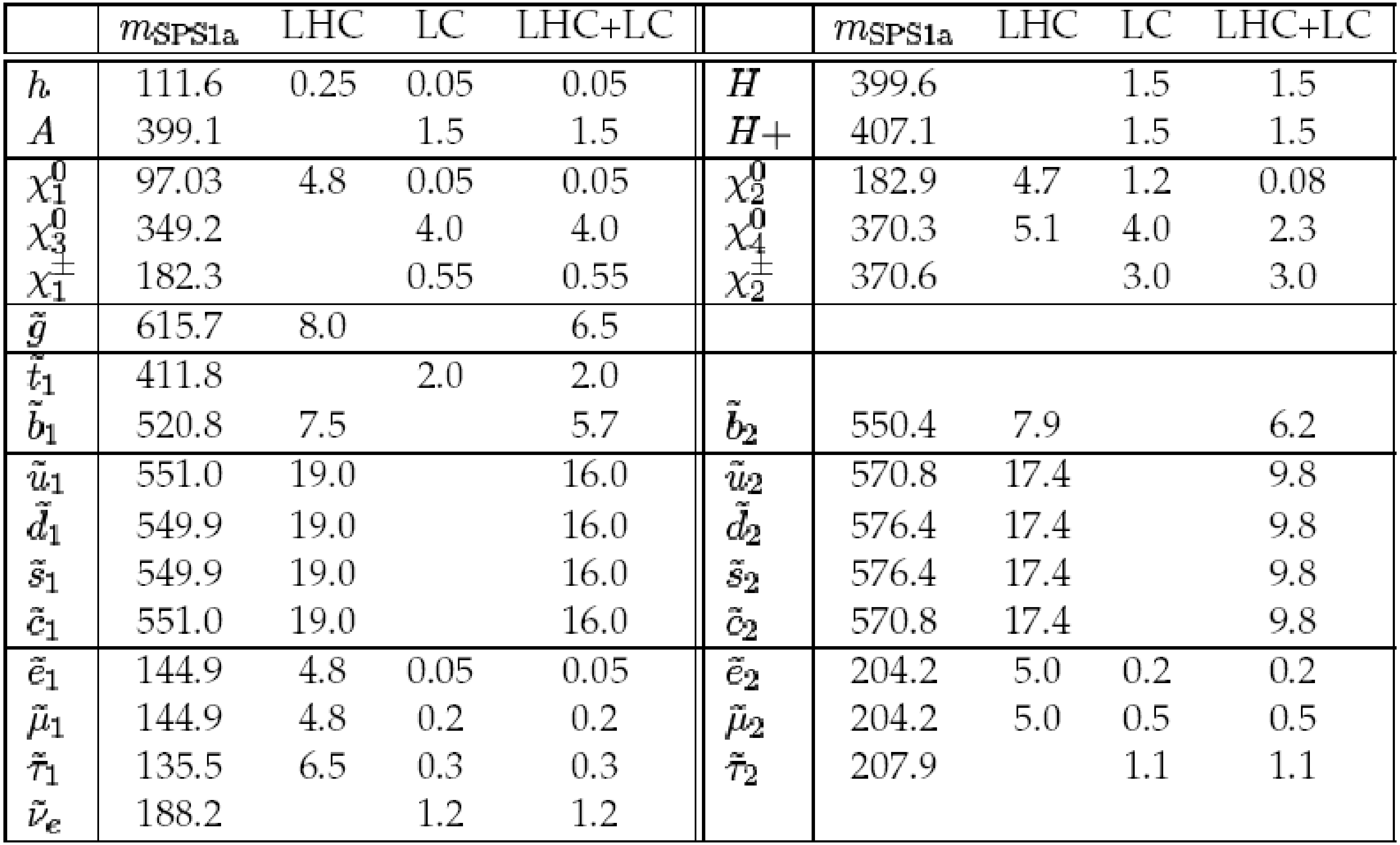

	m_{SPS1a}	LHC	LC	LHC+LC		m_{SPS1a}	LHC	LC	LHC+LC
h	111.6	0.25	0.05	0.05	H	399.6		1.5	1.5
A	399.1		1.5	1.5	$H+$	407.1		1.5	1.5
χ_1^0	97.03	4.8	0.05	0.05	χ_2^0	182.9	4.7	1.2	0.08
χ_3^0	349.2		4.0	4.0	χ_4^0	370.3	5.1	4.0	2.3
$\chi_1^\pm$	182.3		0.55	0.55	$\chi_2^\pm$	370.6		3.0	3.0
$\tilde{g}$	615.7	8.0		6.5					
$\tilde{t}_1$	411.8		2.0	2.0					
$\tilde{b}_1$	520.8	7.5		5.7	$\tilde{b}_2$	550.4	7.9		6.2
$\tilde{u}_1$	551.0	19.0		16.0	$\tilde{u}_2$	570.8	17.4		9.8
$\tilde{d}_1$	549.9	19.0		16.0	$\tilde{d}_2$	576.4	17.4		9.8
$\tilde{s}_1$	549.9	19.0		16.0	$\tilde{s}_2$	576.4	17.4		9.8
$\tilde{c}_1$	551.0	19.0		16.0	$\tilde{c}_2$	570.8	17.4		9.8
$\tilde{e}_1$	144.9	4.8	0.05	0.05	$\tilde{e}_2$	204.2	5.0	0.2	0.2
$\tilde{\mu}_1$	144.9	4.8	0.2	0.2	$\tilde{\mu}_2$	204.2	5.0	0.5	0.5
$\tilde{\tau}_1$	135.5	6.5	0.3	0.3	$\tilde{\tau}_2$	207.9		1.1	1.1
$\tilde{\nu}_e$	188.2		1.2	1.2					

Grand Unification in mSUGRA

SPS1a input parameters: $M_{1/2}$ = 250 GeV, M_0 = 100 GeV, A_0 = -100 GeV, sign(μ) = +, tanβ = 10
$\Rightarrow$ unification at $M_U = 2 \cdot 10^{16}$ GeV

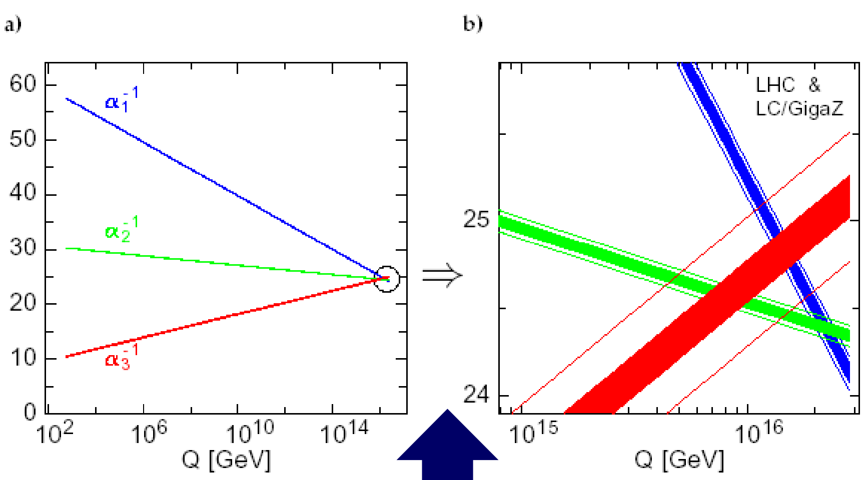

For gauge couplings

For sparticle masses

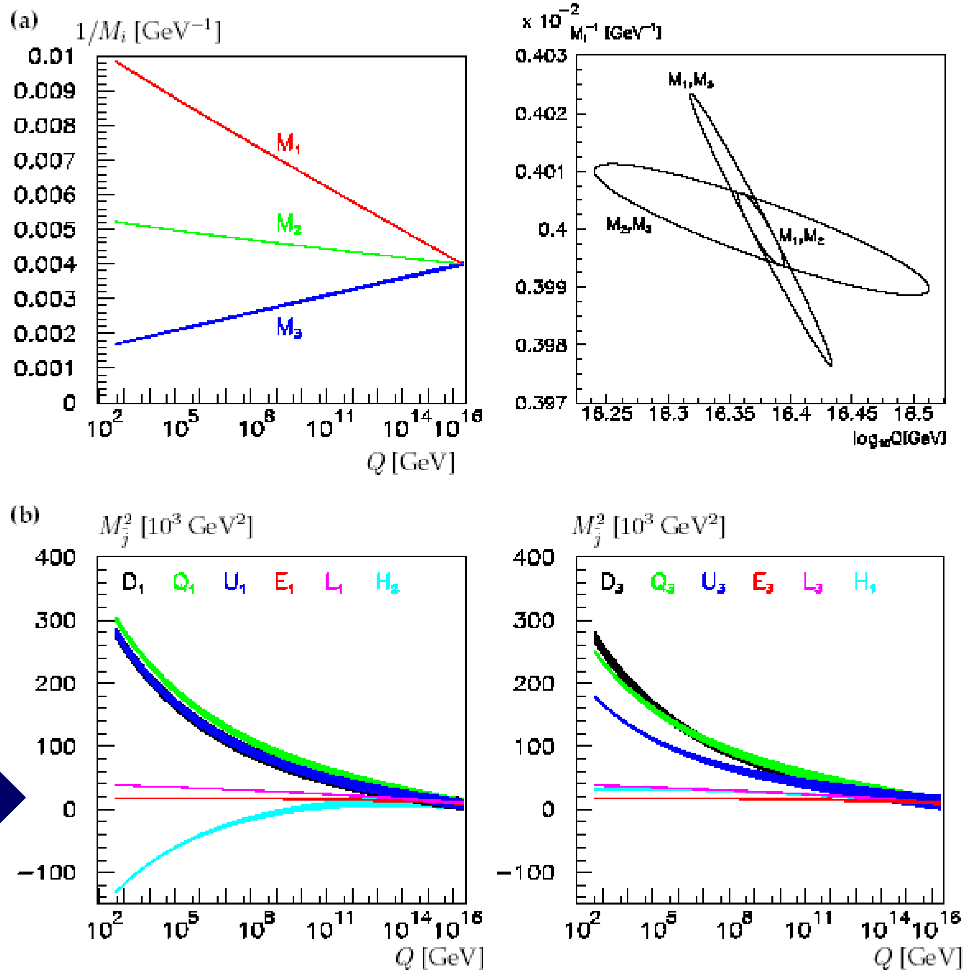

Grand Unification in mSUGRA

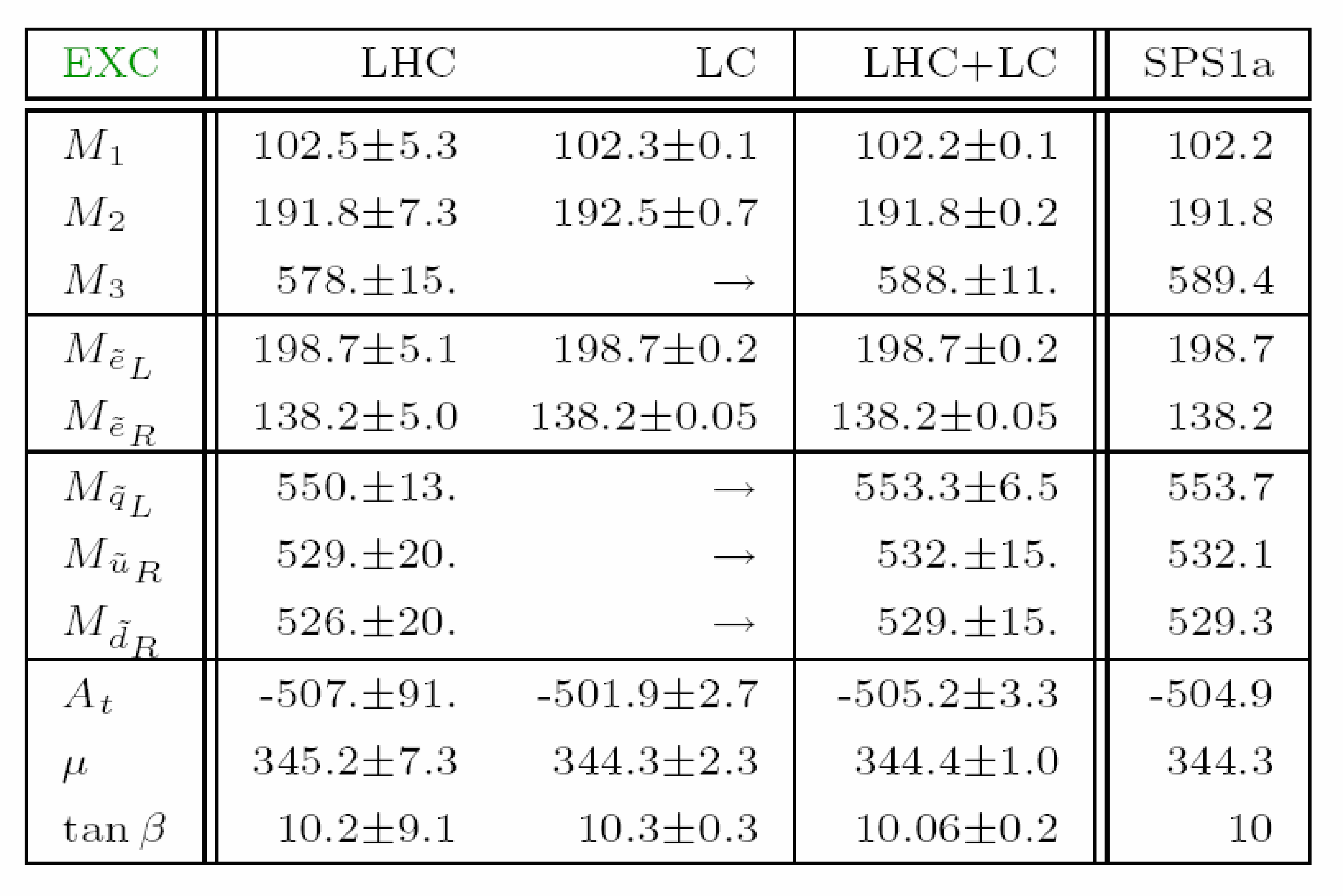

EXC	LHC	LC	LHC+LC	SPS1a
M_1	102.5±5.3	102.3±0.1	102.2±0.1	102.2
M_2	191.8±7.3	192.5±0.7	191.8±0.2	191.8
M_3	578.±15.	→	588.±11.	589.4
$M_{\tilde{e}_L}$	198.7±5.1	198.7±0.2	198.7±0.2	198.7
$M_{\tilde{e}_R}$	138.2±5.0	138.2±0.05	138.2±0.05	138.2
$M_{\tilde{q}_L}$	550.±13.	→	553.3±6.5	553.7
$M_{\tilde{u}_R}$	529.±20.	→	532.±15.	532.1
$M_{\tilde{d}_R}$	526.±20.	→	529.±15.	529.3
A_t	-507.±91.	-501.9±2.7	-505.2±3.3	-504.9
μ	345.2±7.3	344.3±2.3	344.4±1.0	344.3
$\tan\beta$	10.2±9.1	10.3±0.3	10.06±0.2	10

Accelerator

Why a linear collider ?

Energy loss per turn of a machine with an average bending radius r:

$$\Delta E / rev = \frac{C_\gamma E^4}{\rho}$$

Linear Collider: no bends, but *lots* of RF !

For a E_{cm} = 1 TeV machine: Effective gradient *G* = 500 GV / 15 km = 34 MV/m

~15-20 km

Why Super Conducting RF?

- Low RF losses in resonator walls
  (The quality factor: Q_0 ~ RF power stored/RF power lost)
  ($Q_0 \approx 10^{10}$ compared to Cu $\approx 10^4$)
  - high efficiency $\eta_{AC \rightarrow beam}$
  - long beam pulses (many bunches) → low RF peak power
  - large bunch spacing allowing feedback correction within bunch train.

- Low-frequency accelerating structures
  (1.3 GHz, for Cu 6-30 GHz)
  very small *wakefields*
  relaxed alignment tolerances
  high beam stability

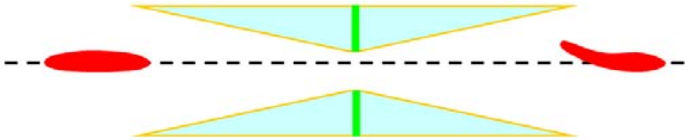

Wakefield: a particle going through an aperture induces charges and currents which produce electromagnetic fields (wake fields) that act on later particles

Compare to a boat travelling in a canal; waves reflected against the boarders of the canal

- Resistive wall wakefield:
  due to finite conductivity of cavities
- Geometric wakefield:
  due to changes in vacuum chamber X-section

TESLA Nine-Cell 1.3GHz Cavity

1 meter length

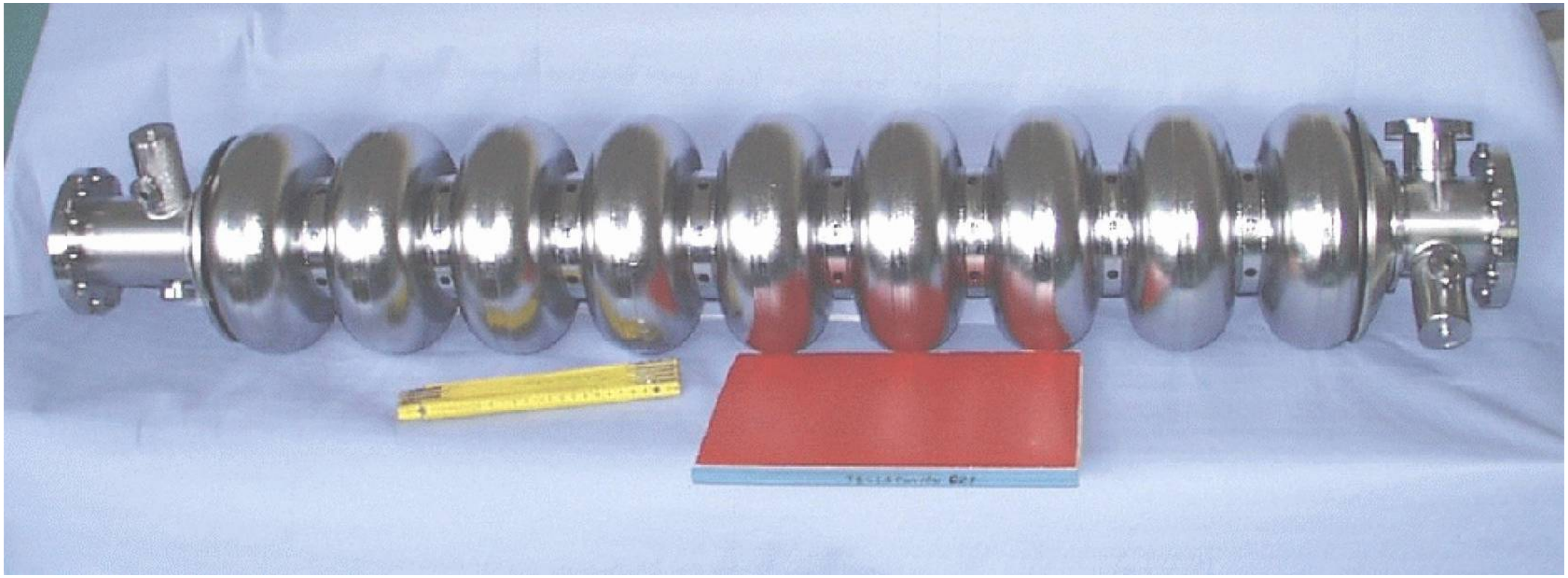

9-cell 1.3GHz Niobium Cavity

ILC Technology Status
Accelerating Structures

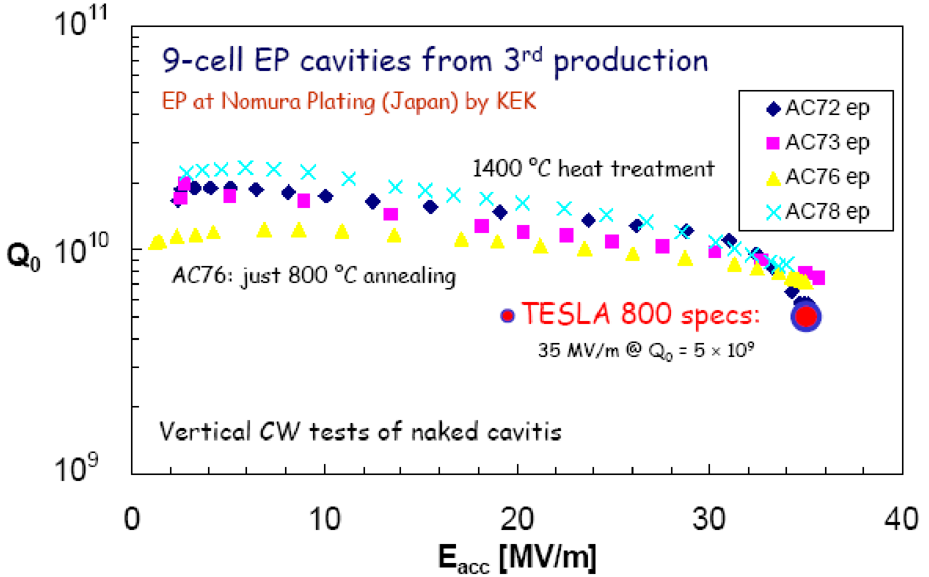

← Vertical (low power test)

Comparison of low and high power tests (AC73) →

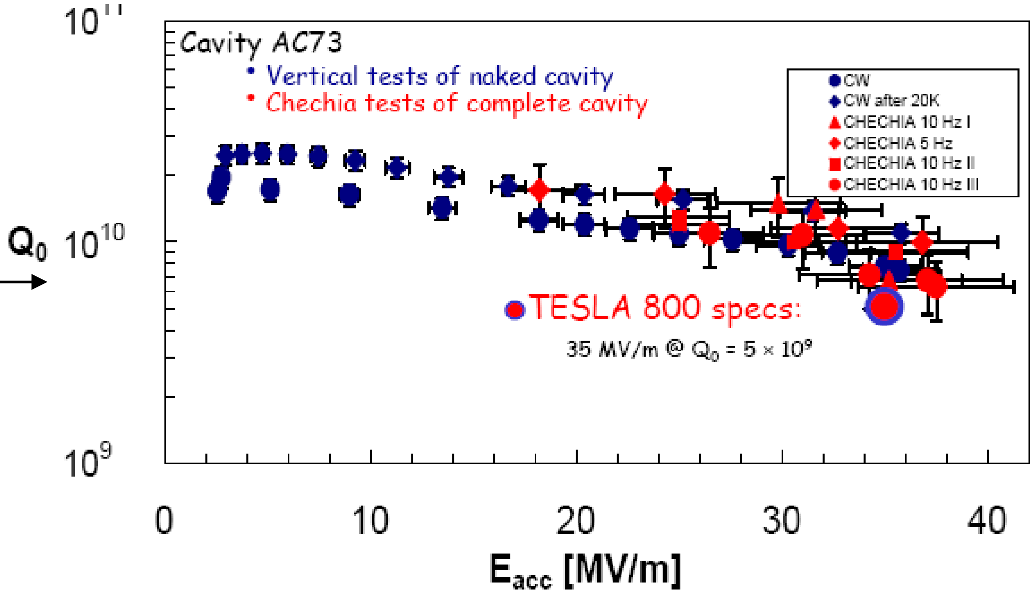

11/03/2008

Possible Minor Enhancement

Low Loss Design

Small modification to cavity shape reduces peak B field.

Increase operation margin.

Increases peak E field ☹ (field emission)

Mechanical stability ?? (Lorentz force detuning)

Baseline
TESLA shape

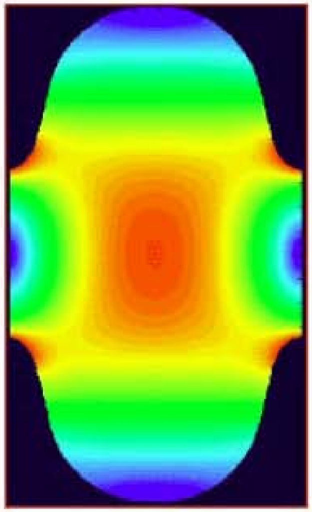

Low Loss Shape
LL

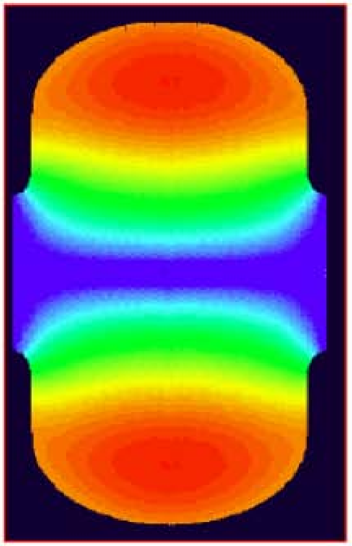

KEK currently producing prototypes

Possible Minor Enhancement

Low Loss Design

Small modification to cavity shape reduces peak B field.

Increase operation margin.

Increases peak E field ☹ (field emission)

Mechanical stability ?? (Lorentz force detuning)

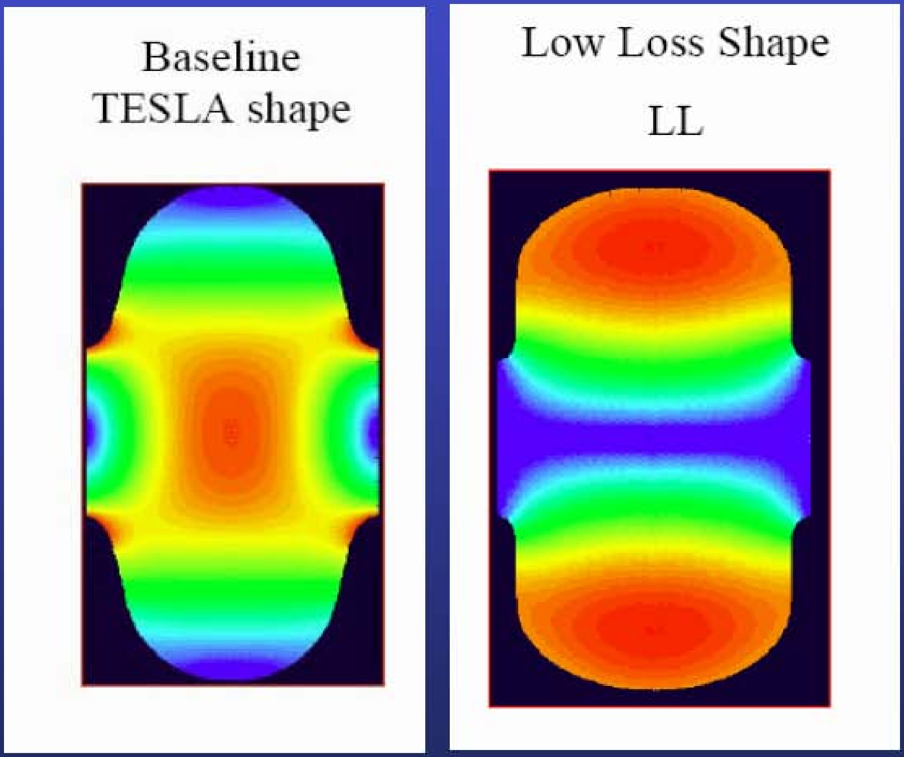

KEK currently producing prototypes

Gradient versus Length

- Higher gradient gives shorter linac ☺
  - cheaper tunnel / civil engineering
  - less cavities
  - (but still need same # klystrons)

- Higher gradient needs more refrigeration ☹
  - ‘cryo-power’ per unit length scales as G^2/Q_0
  - cost of cryoplants goes up!

Simple Cost Scaling

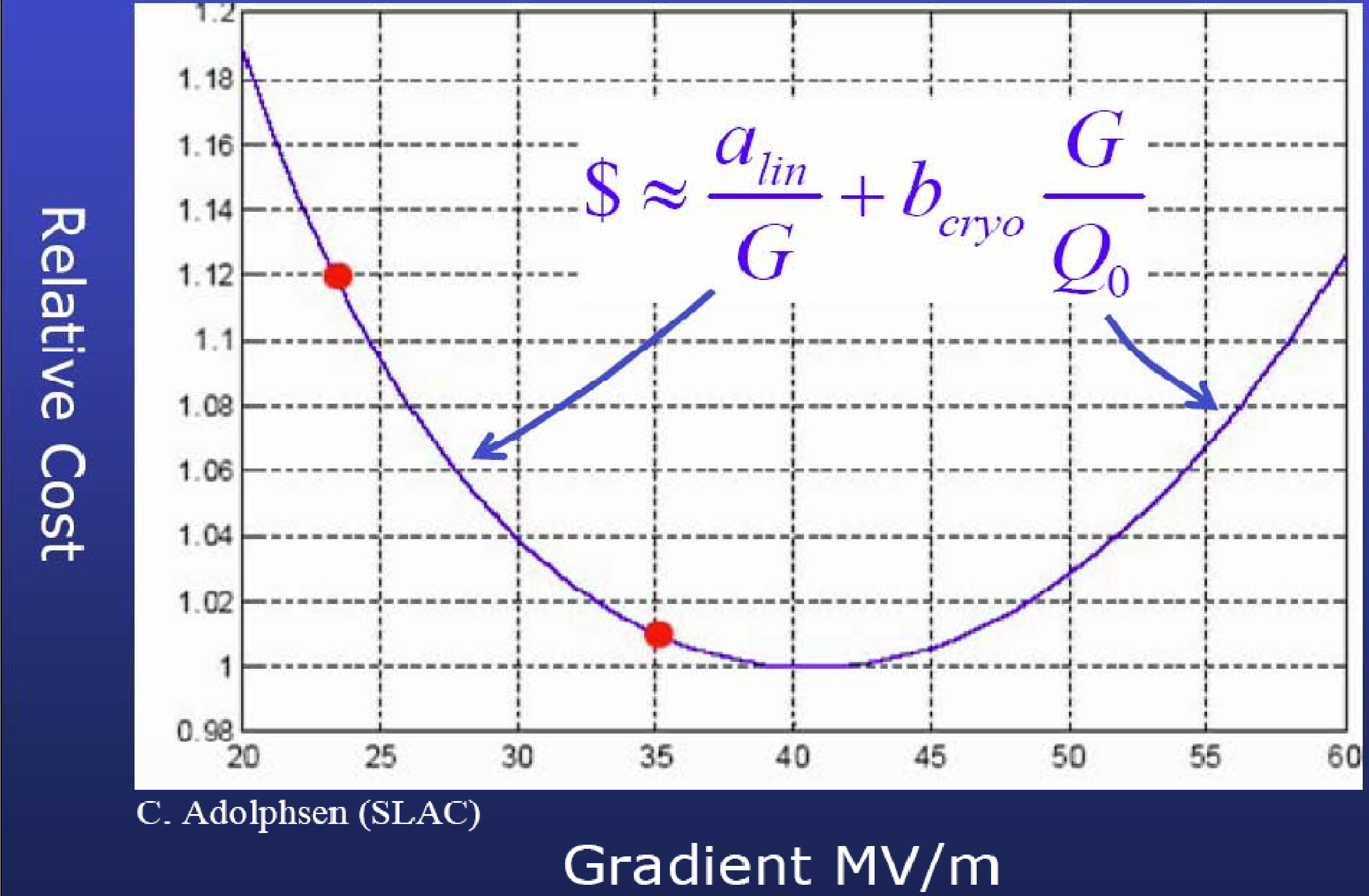

$$\$ \approx \frac{a_{lin}}{G} + b_{cryo}\frac{G}{Q_0}$$

C. Adolphsen (SLAC)

general consensus that 35MV/m is close to optimum

However Japanese are still pushing for 40-45MV/m

30 MV/m would give safety margin

Cryo modules

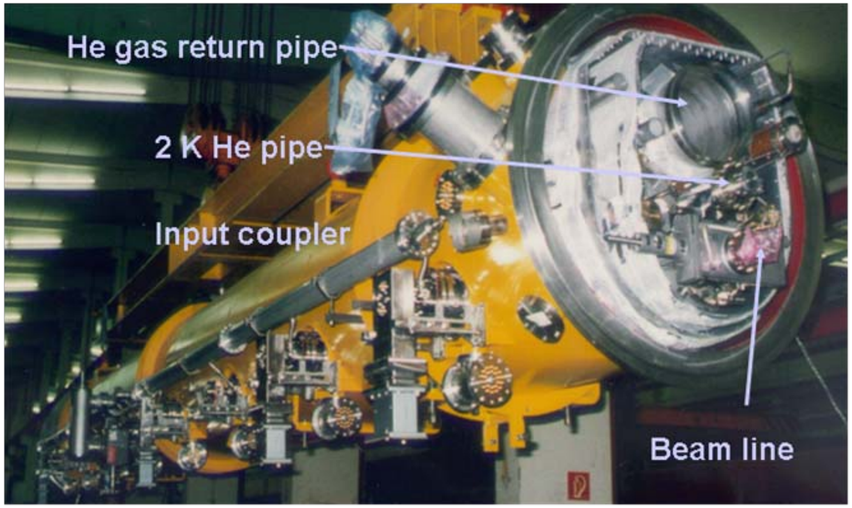

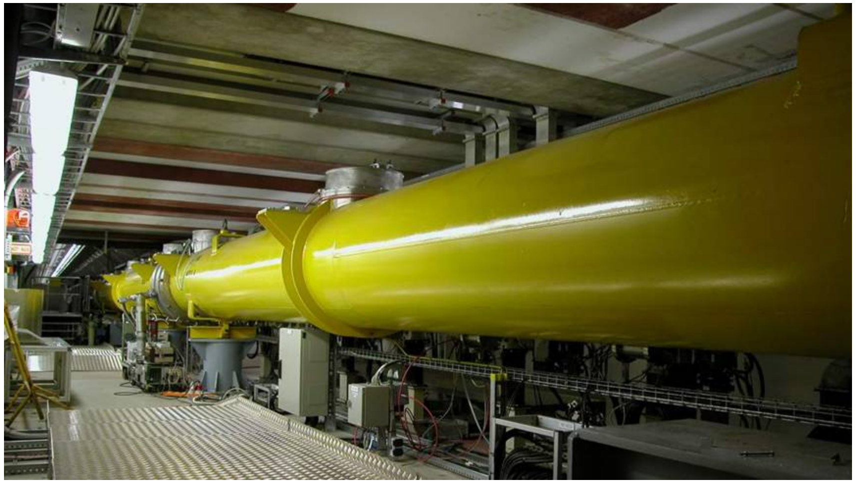

The Main Linac

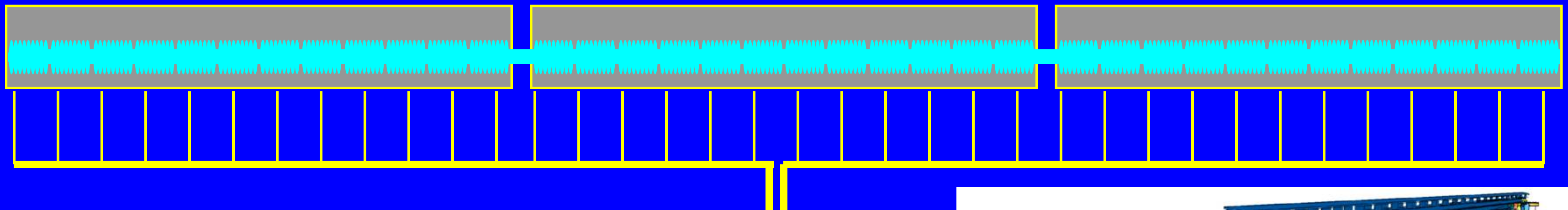

10MW klystron

36 9-cell 1.3 GHz Niobium Cavity

3 Cryomodules

1 10 MW Multi-Beam Klystron

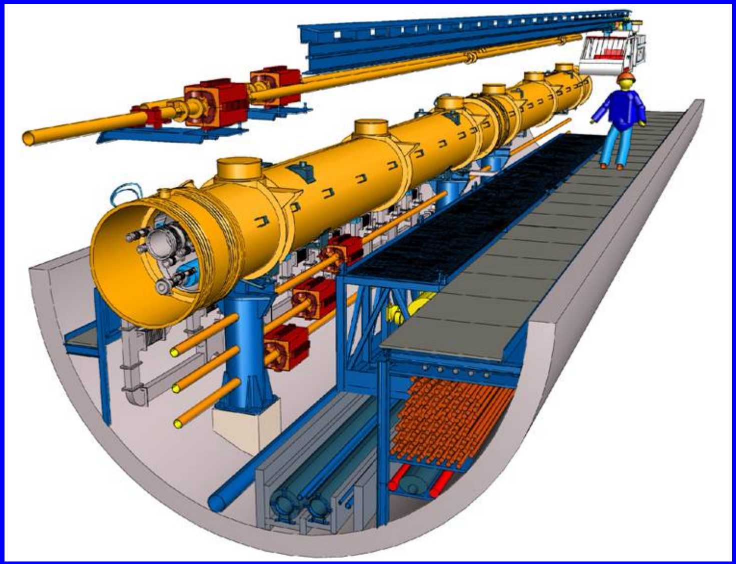

The ILC schematic

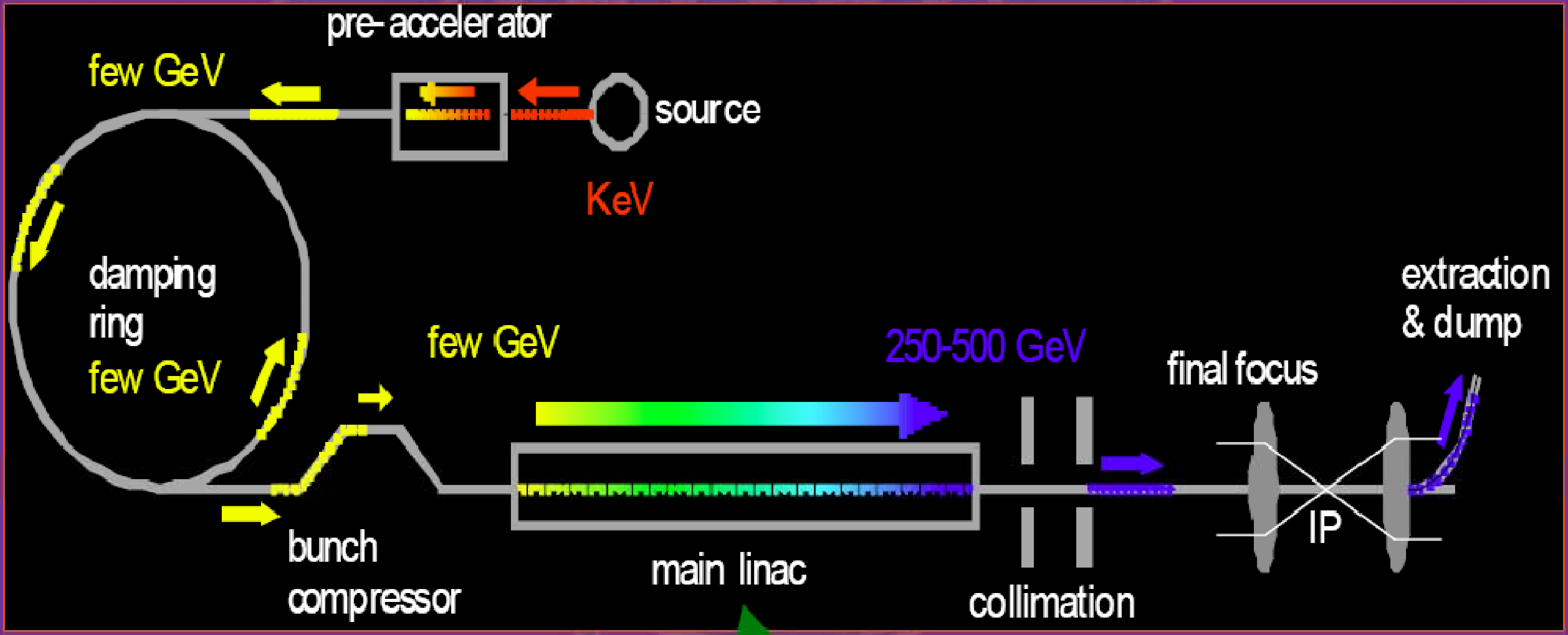

Superconducting RF Main Linac

SCRF Linear Collider

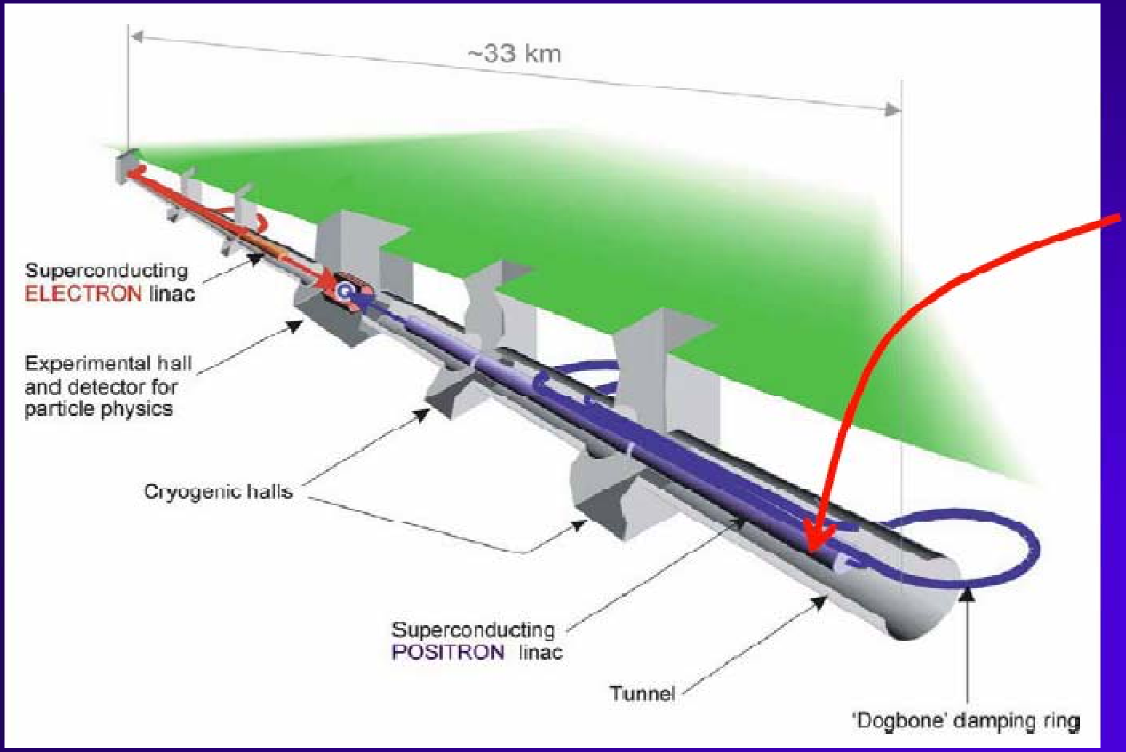

Each linac will have:

~10,000 SCRF cavities

~830 Cryomodules

~280 10MW Klystrons
~280 Modulators

~280 LLRF modules

~350 SC Quadrupoles
~900 power supplies
~350 BPMs + elect.

~3 Large Cryoplants

×2!

The TESLA machine: parameters

Repetition rate :
5 Hz
x 2820 bunches
x 2 $\times 10^{10}$ electrons

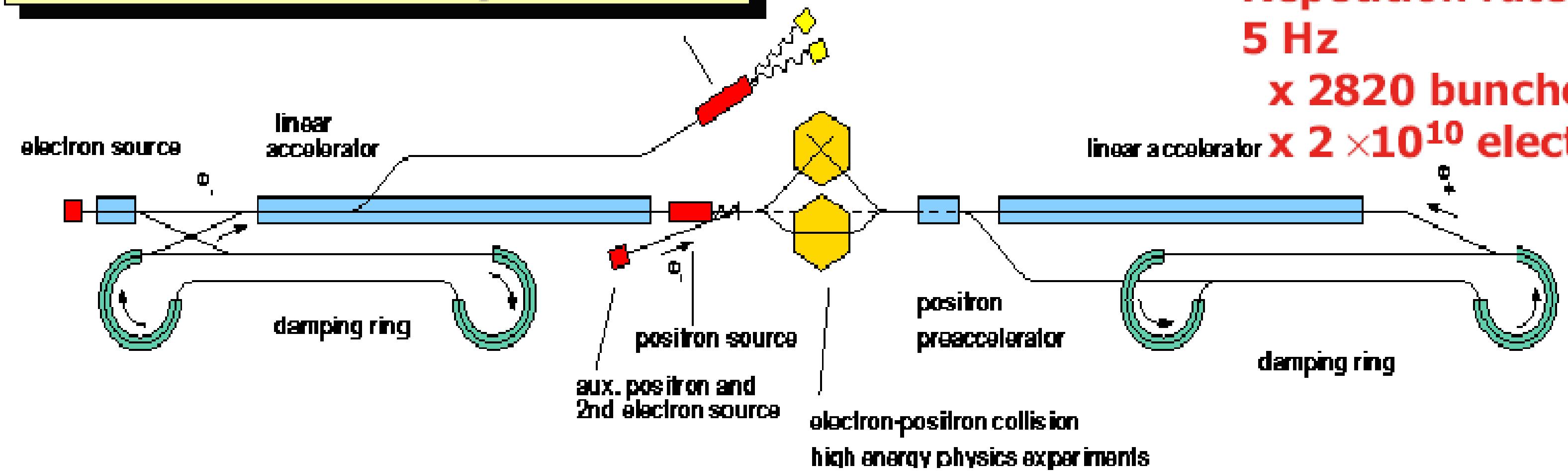

Parameter	TESLA
C.M. Energy [GeV]	500
Luminosity [cm^{-2}/s]	$3.4 \times 10^{+34}$
Beam size σx [nm]	**553**
Beam size σy [nm]	**5**
Bunch length [mm]	**0.3**
Particles per bunch	$2 \times 10^{+10}$
Bunches / train	2820
Bunch interspacing [ns]	337
Repetition rate [Hz]	5
Beamstrahlung [%]	4

The Baseline Machine (500GeV)

January 2006

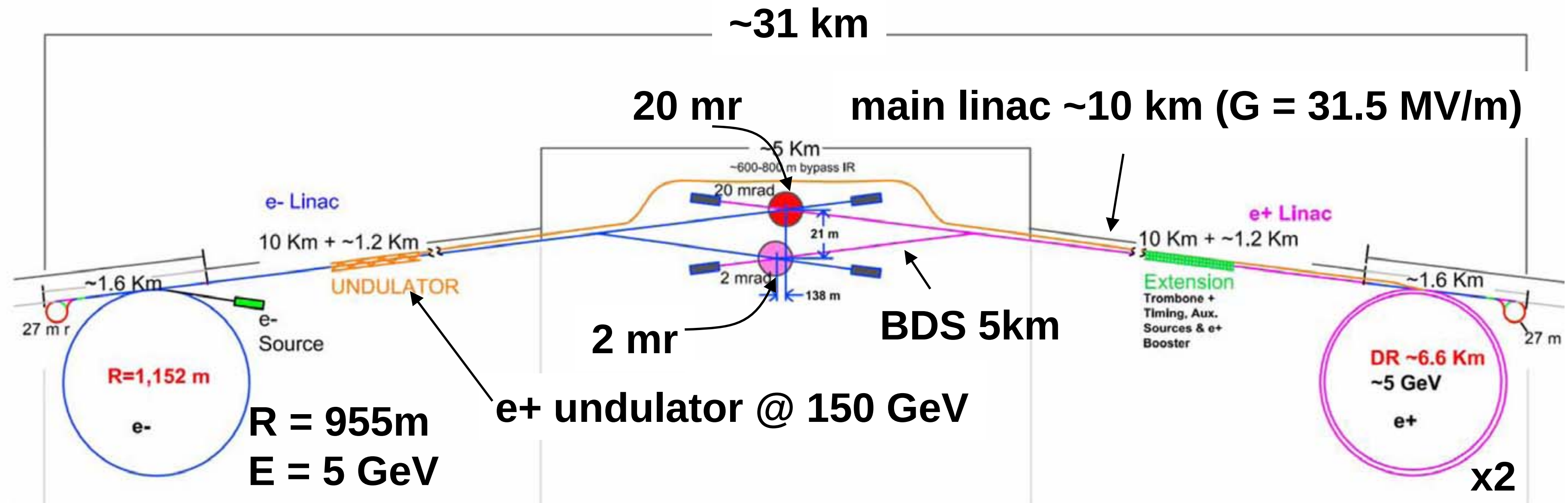

~31 km

20 mr

main linac ~10 km (G = 31.5 MV/m)

2 mr

BDS 5km

e+ undulator @ 150 GeV

R = 955m
E = 5 GeV

x2

not to scale

ILC Reference Design – Feb 2007

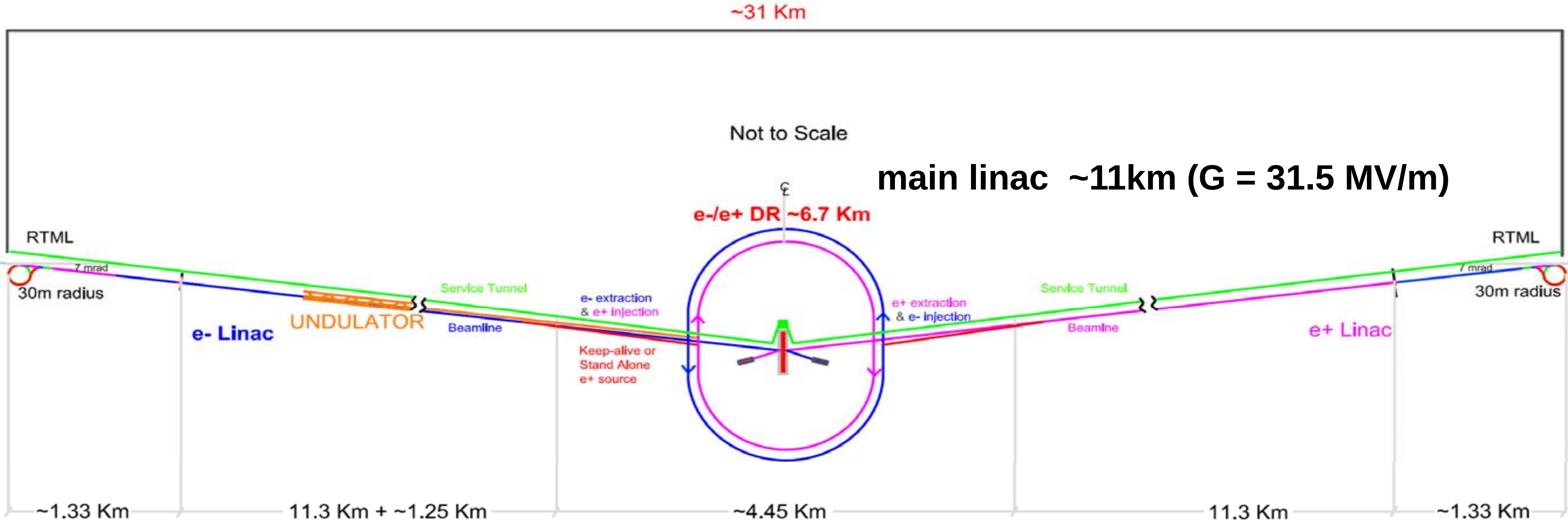

main linac ~11km (G = 31.5 MV/m)

Schematic Layout of the 500 GeV Machine

- Centralized injector incl. damping rings
- Single IR with 14 mrad crossing angle
- 500 GeV center of mass energy
- Dual tunnel configuration for safety and availability

Generic LC Polarized e⁻ Source

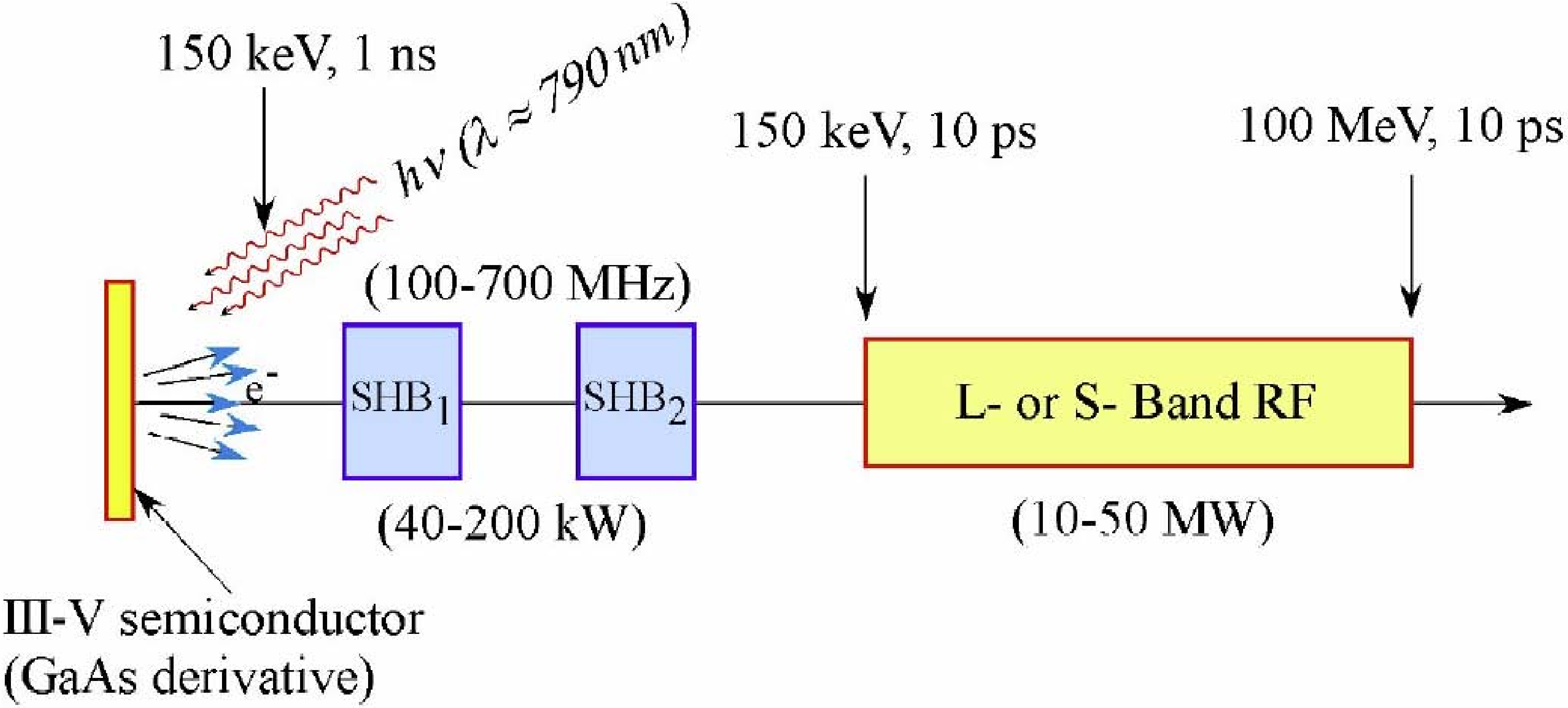

SHB: Subharmonic prebunching cavities
L-band: 0.5 – 1.5 GHz
S-band: 2 - 4 GHz

Positron Source

- Large amount of charge to produce
- Three concepts:
  - undulator-based (TESLA TDR baseline)
  - ‘conventional’
  - laser Compton based

Hotly debated subject.

Undulator-Based

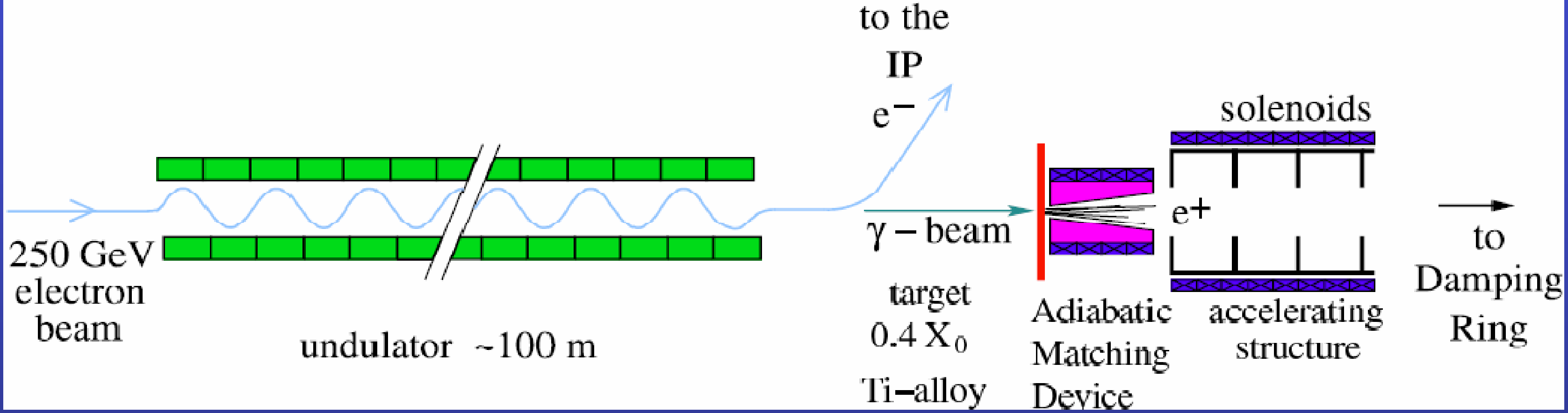

6D e+ emittance small enough that (probably) no pre-DR needed [shifts emphasis/challenge to DR acceptance]

Lower *n* production rates (radiation damage)

Need high-energy e- to make e+ (coupled operation) ☹
Makes commissioning more difficult

Polarised positrons (almost) for free ☺

*Six dimensional cooling based on solenoid magnets surrounding RF cavities

*Emittance: the spread in space and momentum space of a beam

Compton Source (KEK)

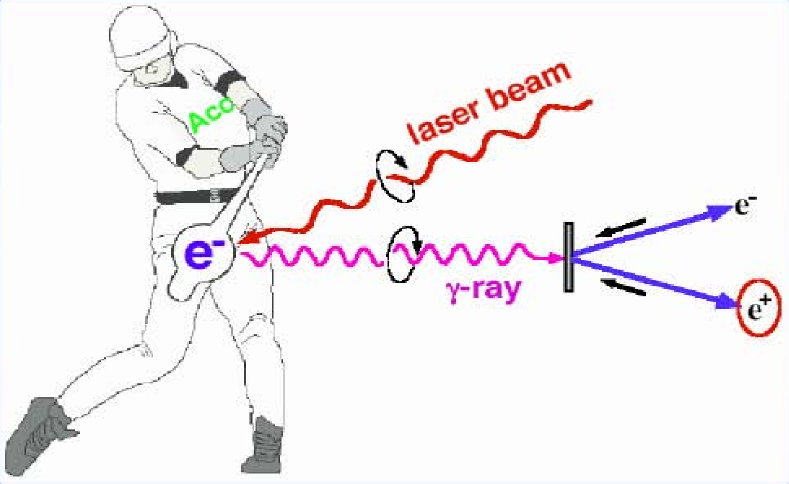

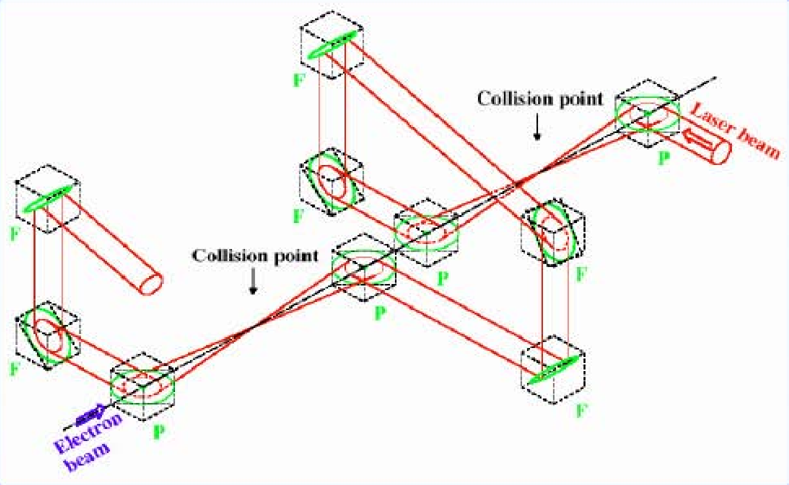

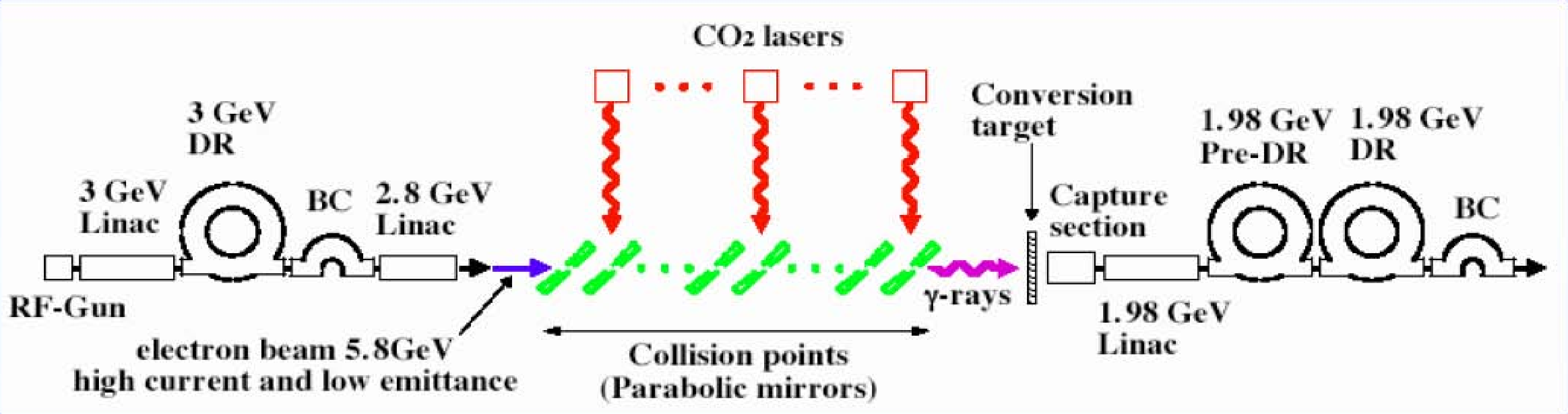

Damping ring

Radiation damping

Principle: - force the electrons to radiate synchrotron radiation, which reduces the momentum spread in all directions
- accelerate the electrons in the desired direction

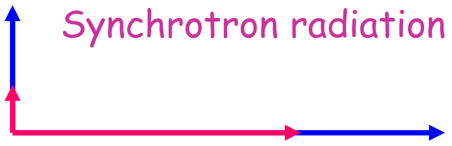

Wiggler magnets: causes the electrons to oscillate transversely

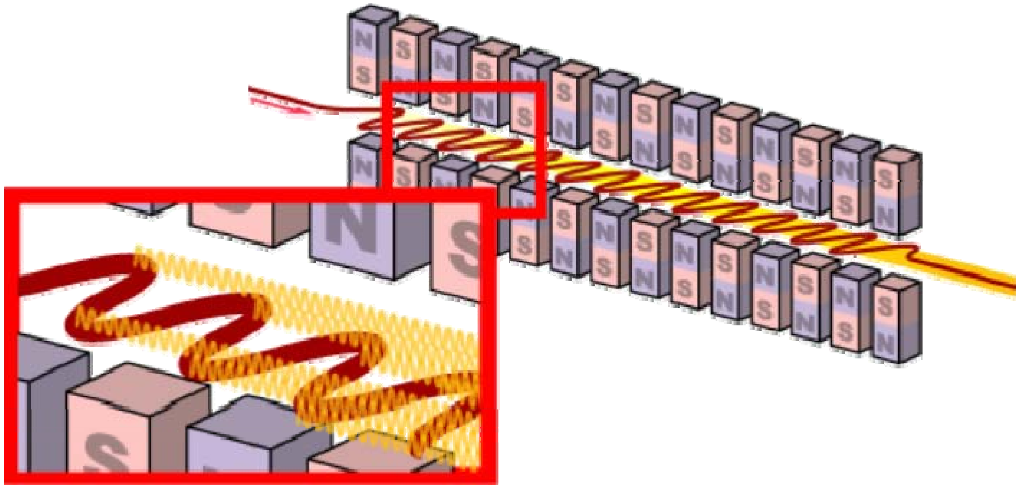

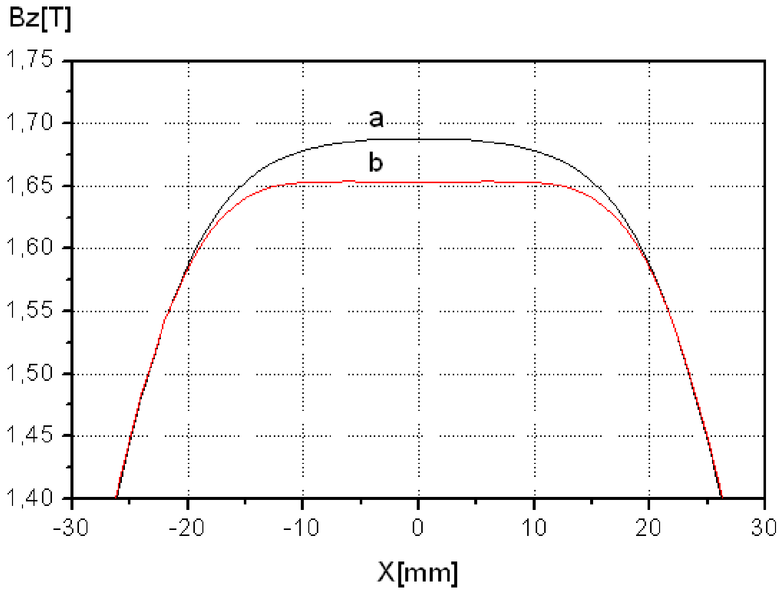

Damping ring

1 ms bunch train → $10^{-3}\text{s} \times 3\cdot10^{8}\text{m/s} = 300$ km ring

DR Design Approaches: Example #1, the TESLA TDR lattice

5 GeV, 17 km lattice (arcs 1 km each, straights 15 km total).

Bunches spaced by 20 ns, injected and extracted individually.

Positron damping ring requires 440 m of wiggler to achieve damping time of 27 ms.

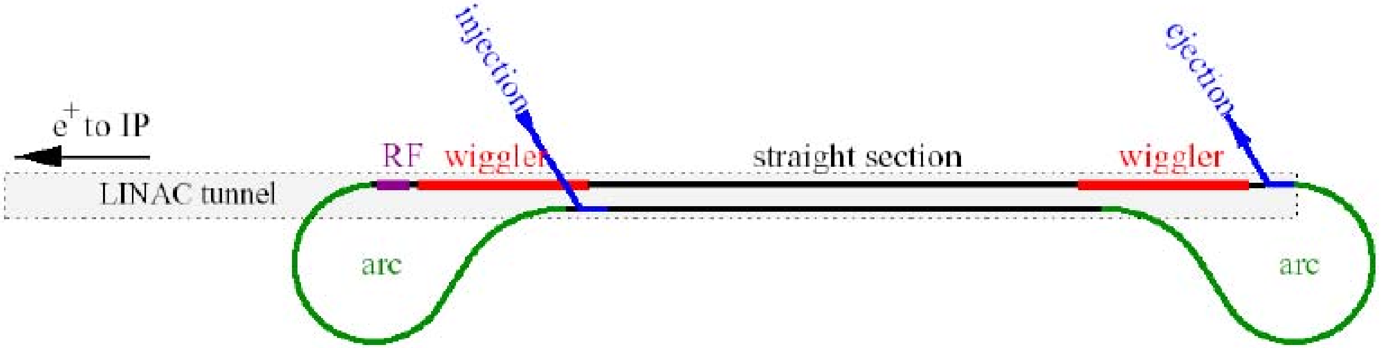

Schematic of Dogbone Damping Ring from TESLA TDR

Strengths:

- Relatively small amount of extra tunnel required.
- Large circumference reduces average current, and helps mitigate some instabilities.
- Flexibility in modes of operation (e.g. could double number of bunches)

Weaknesses:

- Large space-charge tune shift needs to be corrected using coupling-bumps.
- Sensitive to stray magnetic fields.

Fast feedback

Long bunch train ~ 3000 bunches over 1 ms ⇒ 337 ns between bunches
Multiple feed back system will be mandatory to maintain the nanobeams in collisions

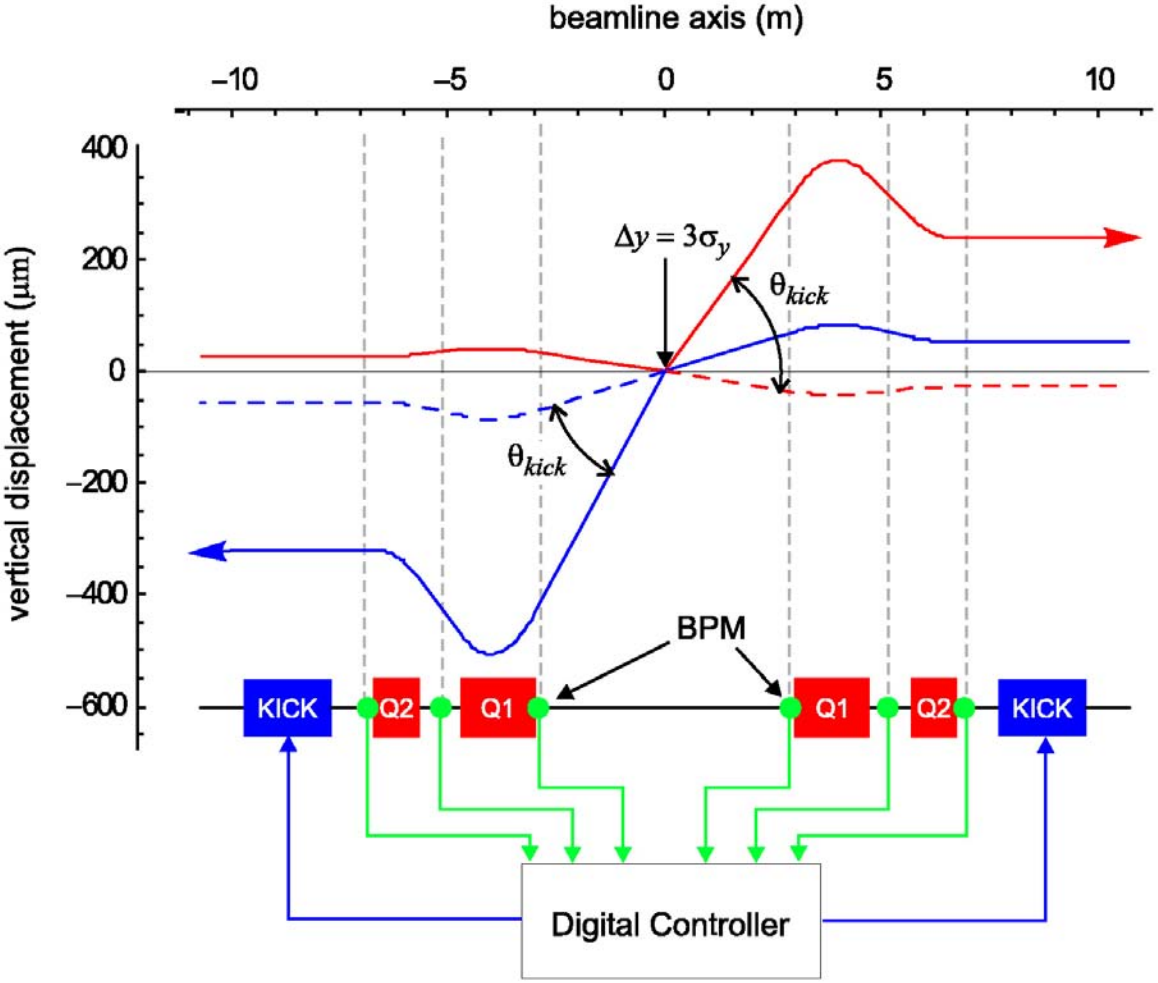

TESLA IP Feedback

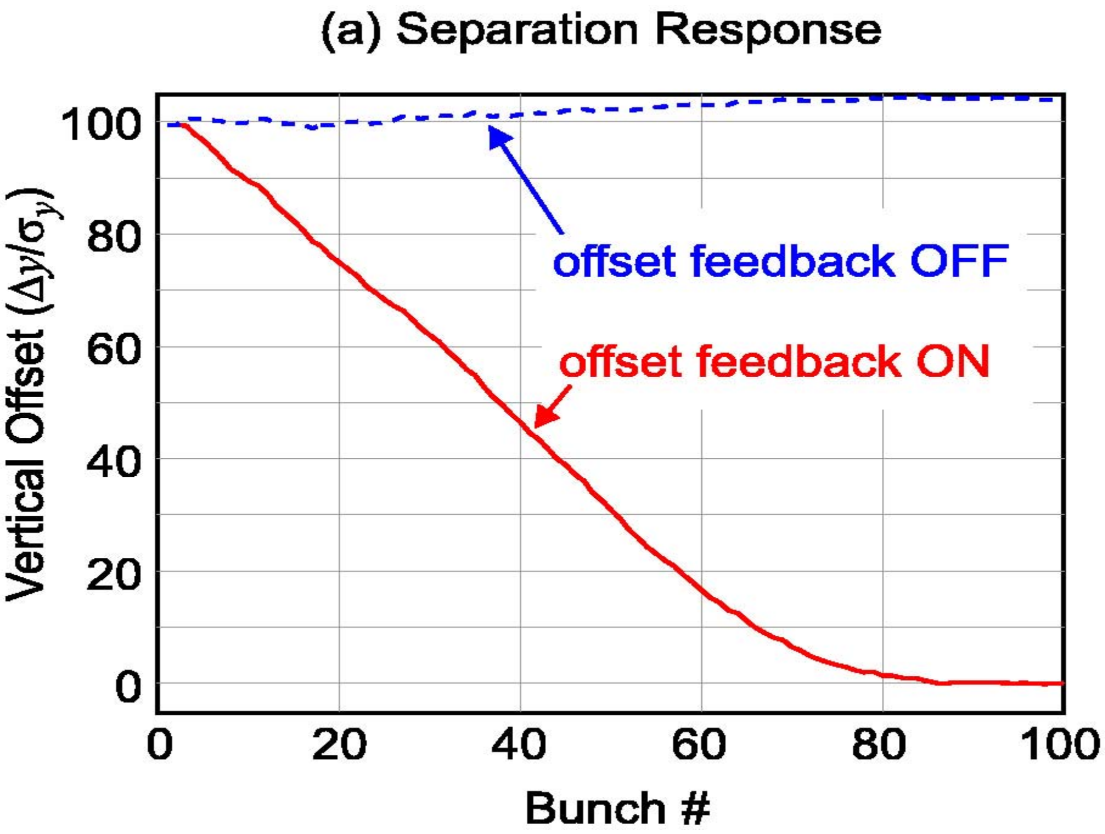

Data aquisition

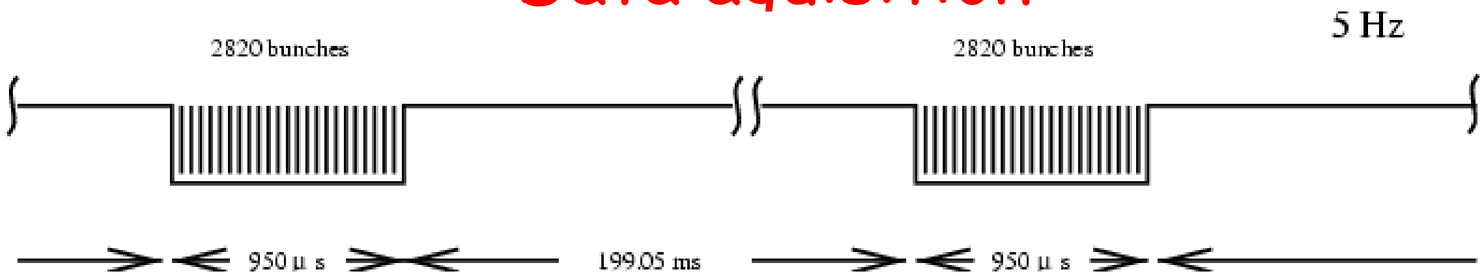

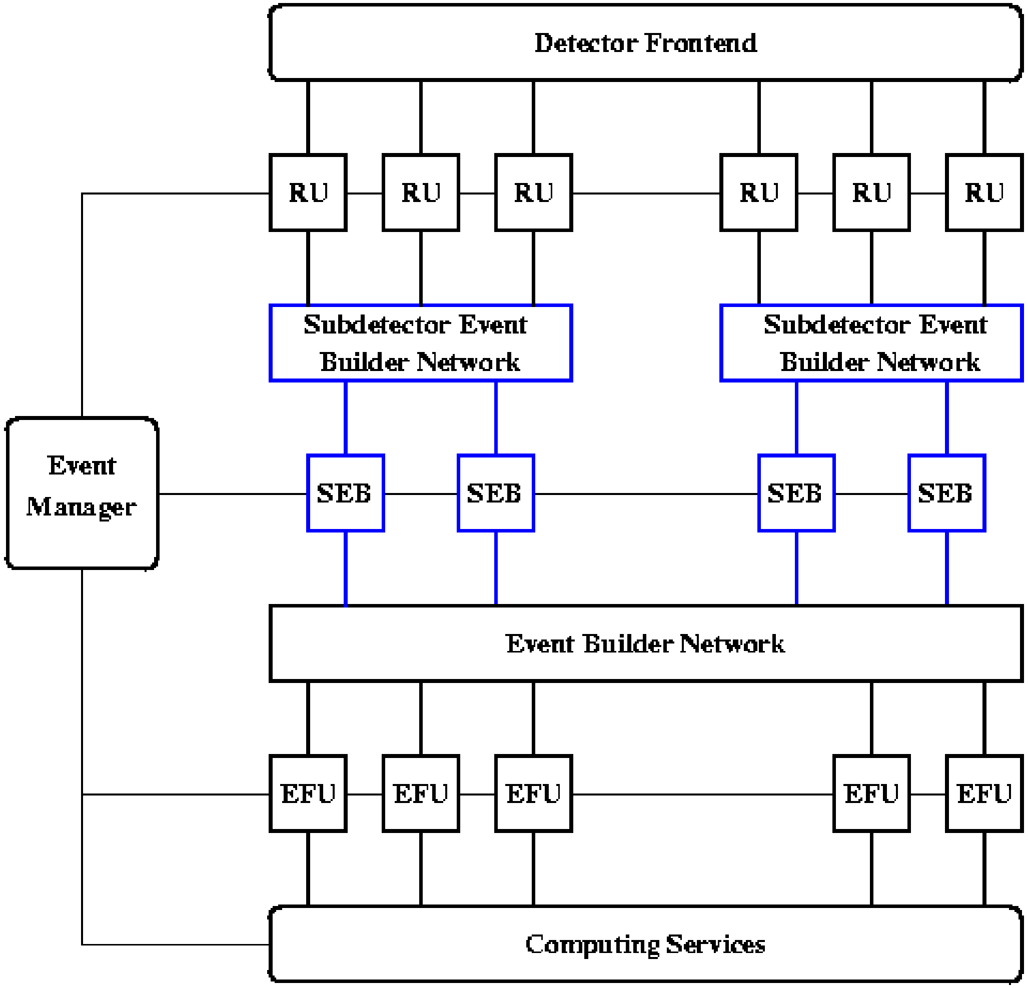

up to 1 ms active pipeline (full train),
no trigger interrupt,
sparcification/cluster finding at FE
standardized readout units (RU)

readout between trains (200ms)

optional subdetector event building

event building network and farm
complete train into a single PC !!

software event selection using
full information of a complete train
define 'bunches of interest'
move data only once into PC
and relevant data to storage

ILC Projected Time Line

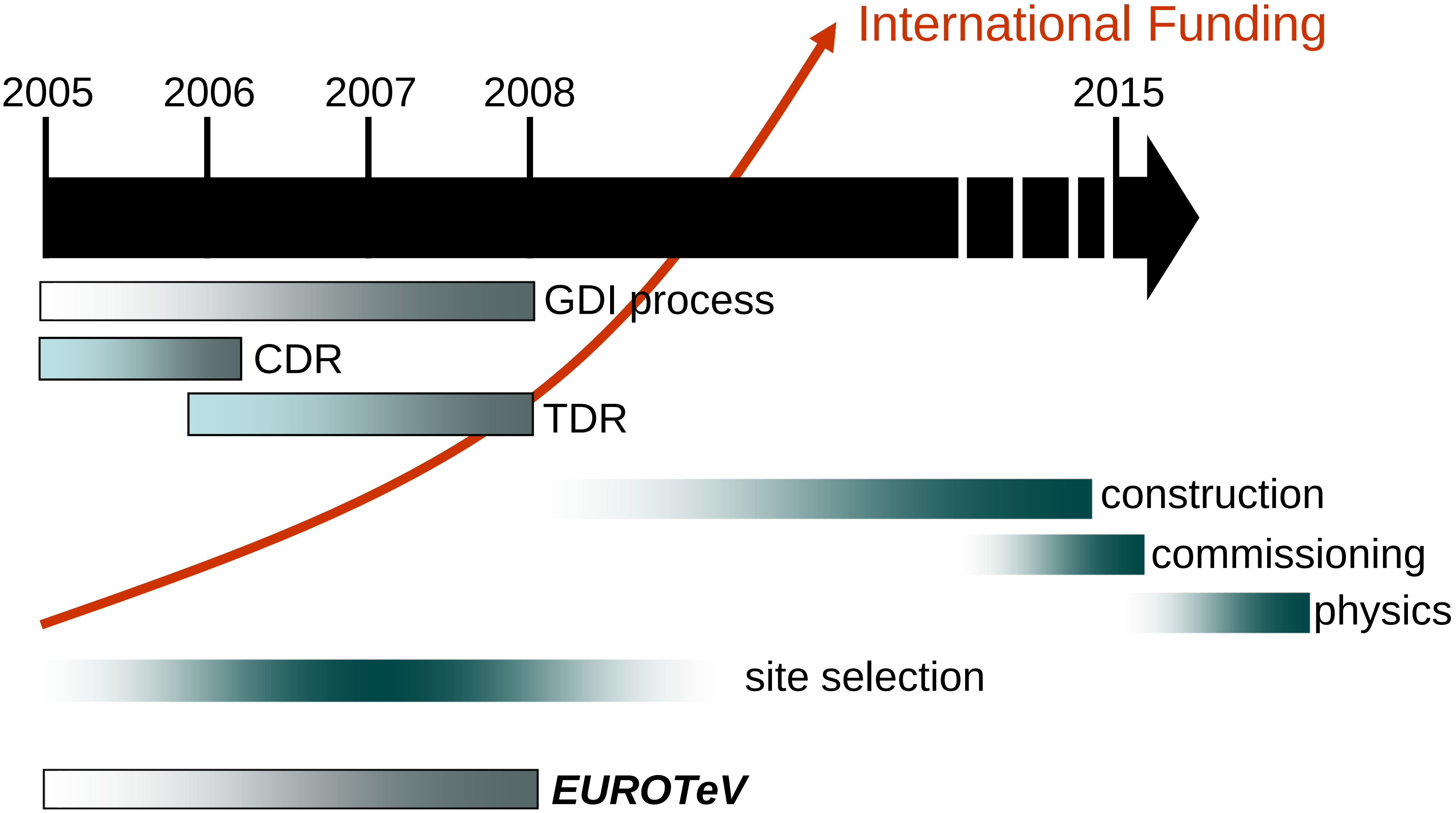

International Funding

2005 2006 2007 2008 2015

GDI process

CDR

TDR

construction

commissioning

physics

site selection

EUROTeV

Very aggressive!

The Global Design Effort GDE

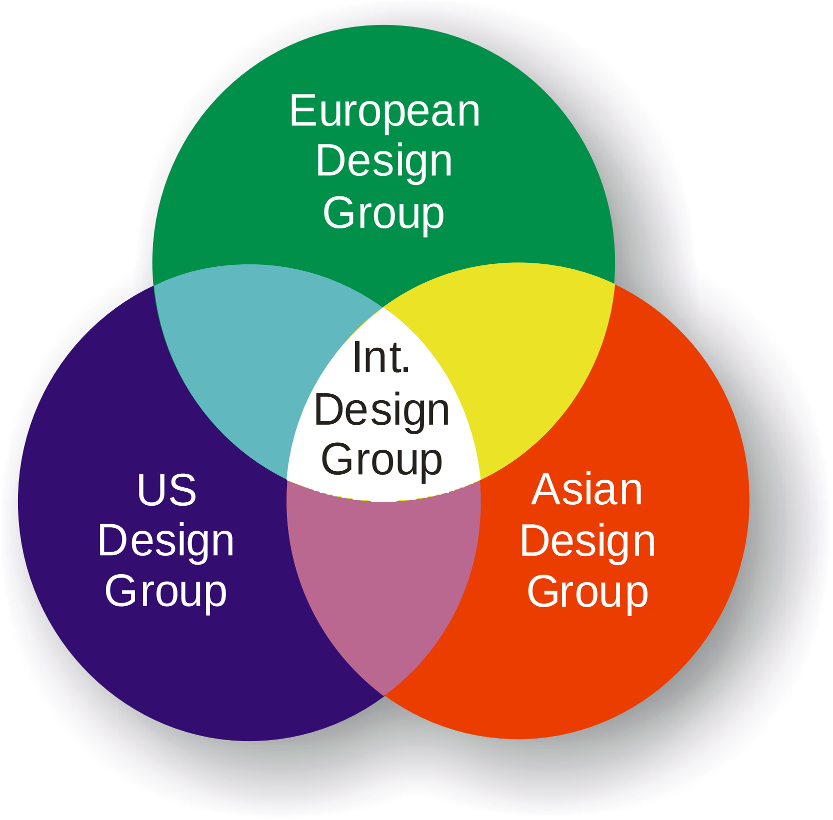

- 3 Regional Design Teams
- Central Group with Director
- Goal: Produce an internal full costed ILC Technical Design Report by 2008

Detector

The detector

The TESLA detector: general layout

(Design proposed for the TESLA TDR)

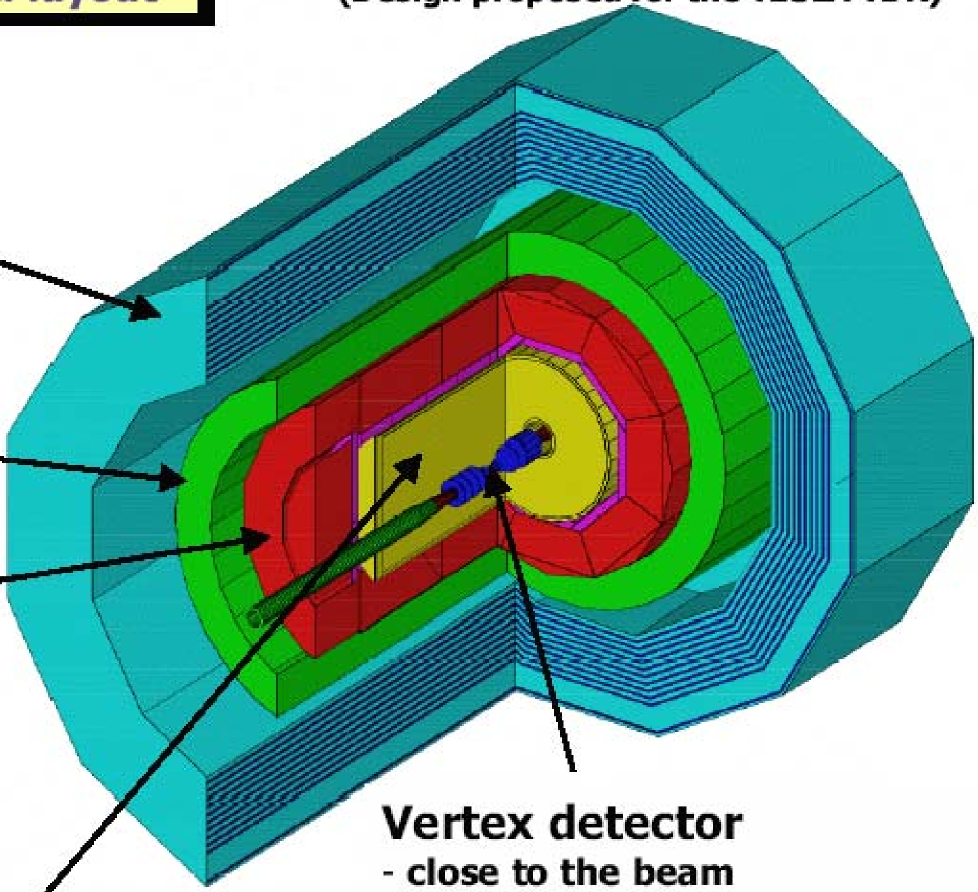

Muon detector

Coil
B = 4 Tesla

Calorimeter
- fine 3D granularity
- very good energy flow

Time Projection Chamber
- **Low amount of material [gas]**
- **Large number of 3D points**
  - → **precise tracking**
  - → **excellent momentum resolution**

Vertex detector
- **close to the beam**
- **reconstruction of secondary vertices of b and c quark decays**

One quadrant side view

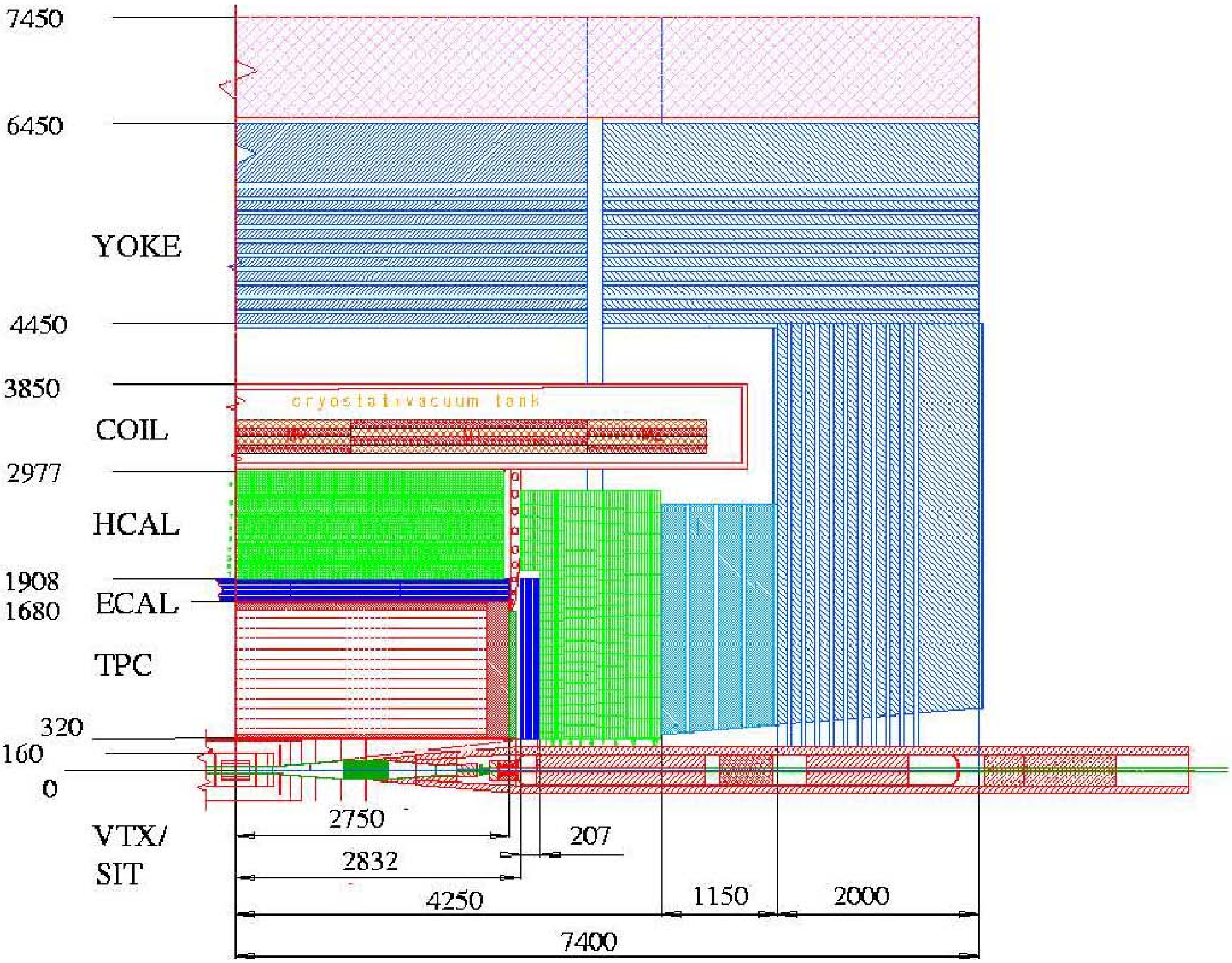

The vertex detector

- vertexing: $\sigma_{r\phi,z}(ip) \leq 5\,\mu\mathrm{m} \oplus \frac{10\,\mu\mathrm{m}\,\mathrm{GeV/c}}{p\sin^{3/2}\theta}$,

  ($1/5\ r_{\mathrm{beampipe}}$, 1/30 pixel size, 1/30 thin w.r.t LHC)

Precision measurements require:

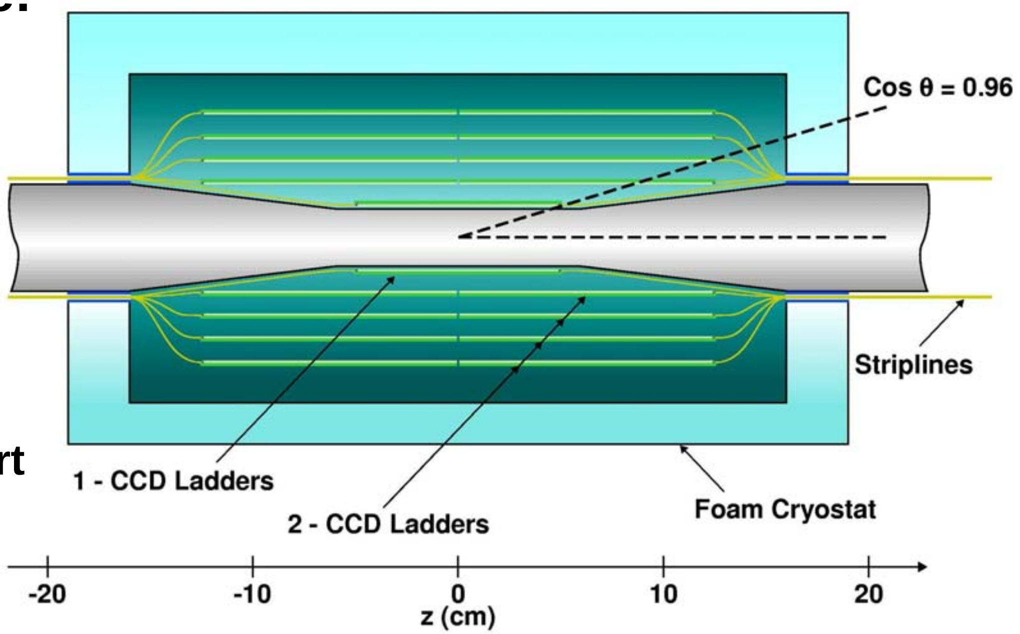

- good angular coverage (cos θ = 0.96)
- proximity to IP, large lever arm:

  5 layers, radii from 15 mm to 60 mm
- minimal layer thickness (< 0.1% X_0)

  to minimise multiple scattering
- mechanically stable, low mass support
- low power consumption

High hit density near interaction point requires:

- small pixel size: 20 μm × 20 μm
- fast readout:

1. Vertex Detector

Occupancy → pixel devices needed.

- Pixel size $\sim 20 \times 20\mu\text{m}^2$.
- Occuancy $\sim$ 0.3% for track matching.
- One should be able to read it out (non-trivial, as it turns out).

Candidates :

- CCD (Charge-Coupled Device)
- HAPS (Hybrid Pixel Sensors)
- MAPS (Monolithic Active Pixel Sensor), FAPS (Flexible -), Small-pixel MAPS ($5 \times 5\mu\text{m}^2$)
- DEPFET (DEPleted Feild-Effect Transistor) SOI (Silicon On Insulator)
- ISIS (Image Sensor with In-situ Storage)

The TPC

- central tracking: $\sigma(\frac{1}{p_t}) \leq 5 \times 10^{-5}(\mathrm{GeV/c})^{-1}$
  (~ 1/10 LHC. 1/6 material in tracking volume.)

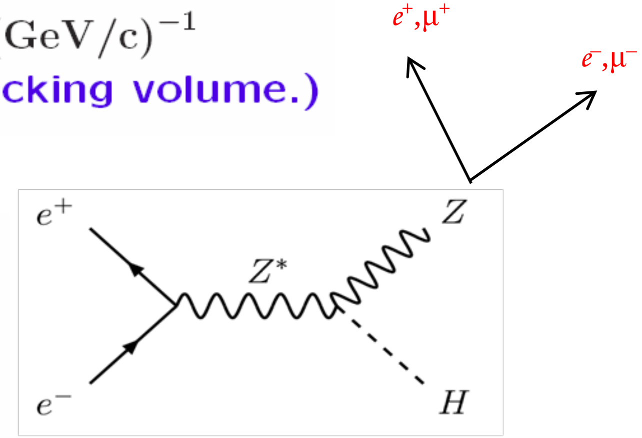

e.g: The Higgs tagging mode

$$e^+e^- \rightarrow ZH, \quad Z \rightarrow \ell^+\ell^-$$

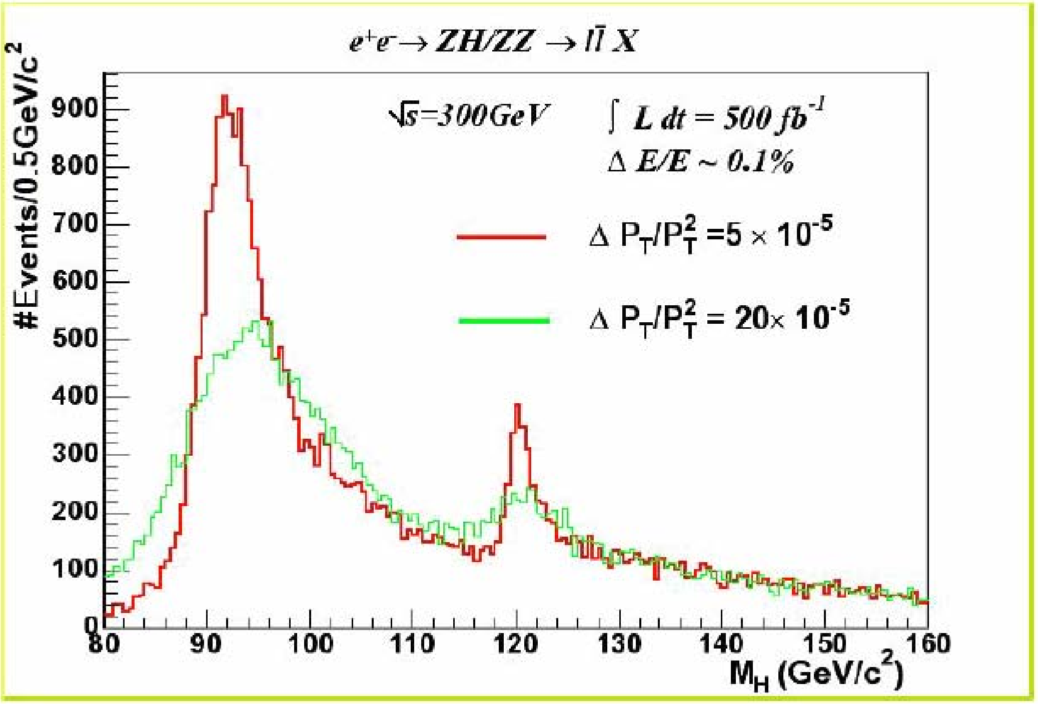

$\frac{\sigma_p}{p^2} \sim 5 \times 10^{-5}$ is 'necessay'.

TPC read-out devices:

Conventional: MWPC + pads
-Positive ion feedback
-Resolution limited by the MWPC response

MPGD's (Micro Pattern Gas Detectors):
-GEM (Gas Electron Multiplier)
-MicroMEGAS (Micro Mesh GAS detector)

TPC as the central tracker at TESLA: Gas amplification: wires

For the drifting electron amplification several solutions are considered:

Wires

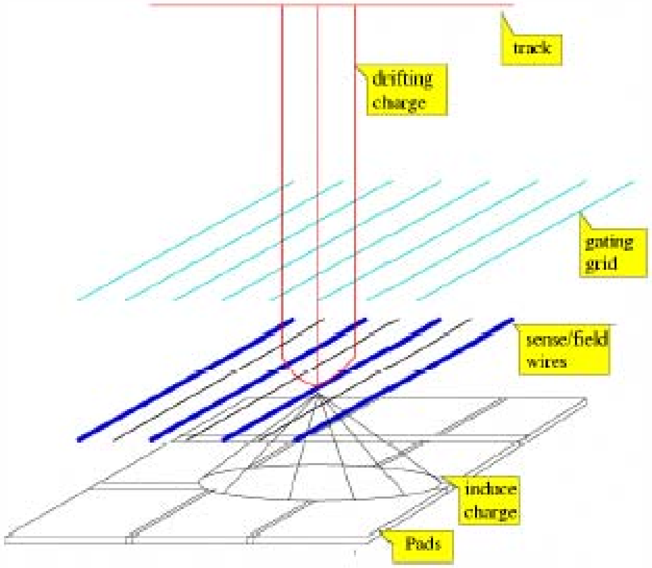

Principle

- primary electrons
- amplification
- signal, induced on the pads
- gating plane for ion feedback reduction

Advantages

- known technology (e.g. TOPAZ, ALEPH, DELPHI, etc...)

But

- high magnetic field
- ion feedback needs gating after every bunch crossing?
- E x B effects

TPC as the central tracker at TESLA: Gas amplification: GEM

Gas Electron Multiplier (F. Sauli et al., 1997)

- thin polymer base (~50 μm)
- coated on each side by ~ 5 μm copper.
- perforated by a high density of small holes
  - 70 μm holes, 100 μm pitch
- Strong field (~ 80 kV/cm) between the two conductive sides.

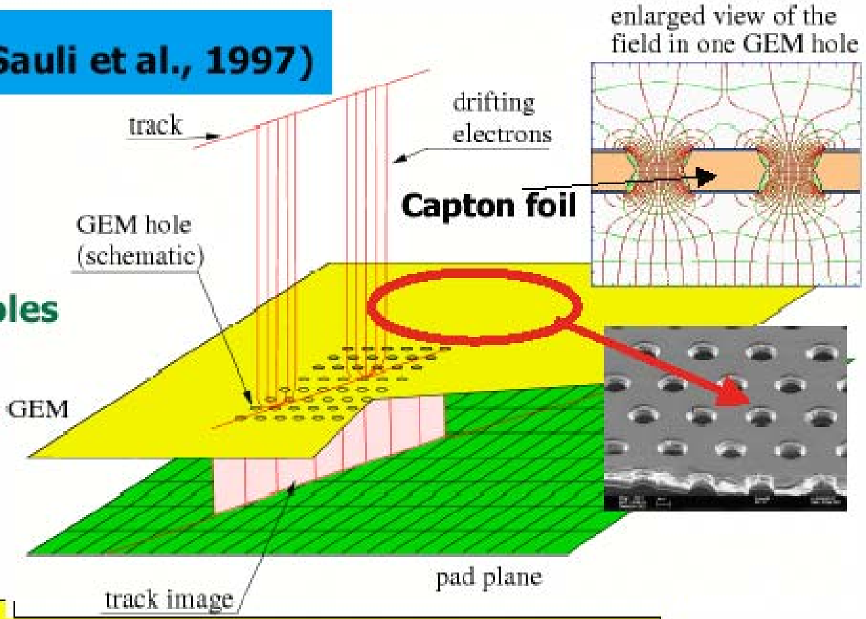

Advantages of GEM:

- almost no E x B effects (~ 50 μm)
- natural suppression of ion feedback
- low material budget
- 2-D symmetry
- high gain and possibility to use multi GEM structure
- fast signal collection
- simple design (no mechanical tension)

TPC as the central tracker at TESLA: Gas amplification: MicroMegas

MicroMegas (Y. Giomataris et al., 1996)

- thin metallic mesh held by dielectric support
- amplification gap~ 100 µm
- high field in the gap ~ 40 kV/cm

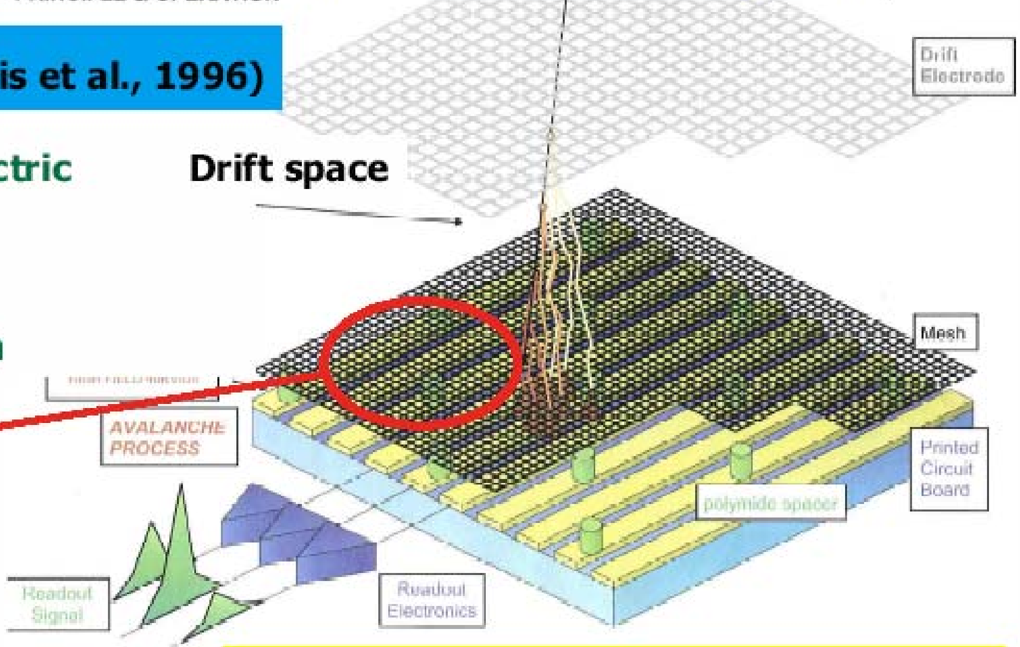

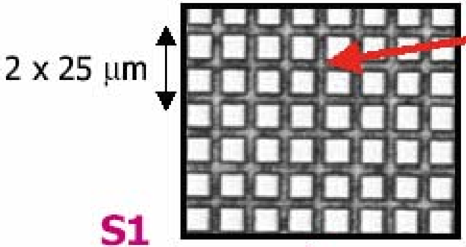

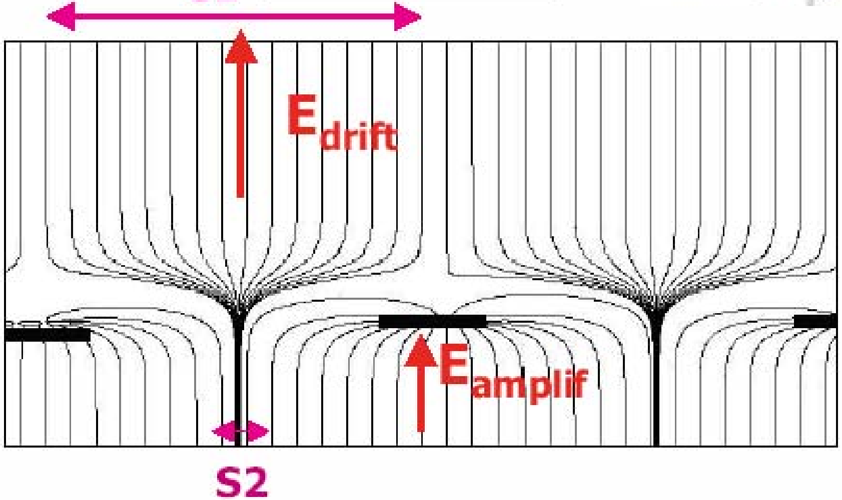

Same advantages as GEM

- large gains (10^3-10^4)
- Funnel effect → efficient ion collection

$$S1/S2 \sim E_{amplif} / E_{drift}$$

Ions are unlikely to follow the field lines and return to the drift volume.

Ions return to the grid

The electromagnetic calorimeter

• Si-W calorimeter: (tracking calorimeter)	High granularity (~ 1x1 cm^2) Expensive Segmentation optimization (cost reduction)
• Tile fibre calorimeter:	Modest granularity (4x4 cm^2) Segmentation optimization? Fibre configuration?
• Shashlik calorimeter:	Fibres run longitudinally Longitudinal segmentation? Scintillating fibre type?
• Scintillator strip calo:	Orthogonally arranged

- Typical energy resolution: $\Delta E/E = 10 - 15\%/\sqrt{E}$

One of the jets in a 2-jet event at 91 GeV

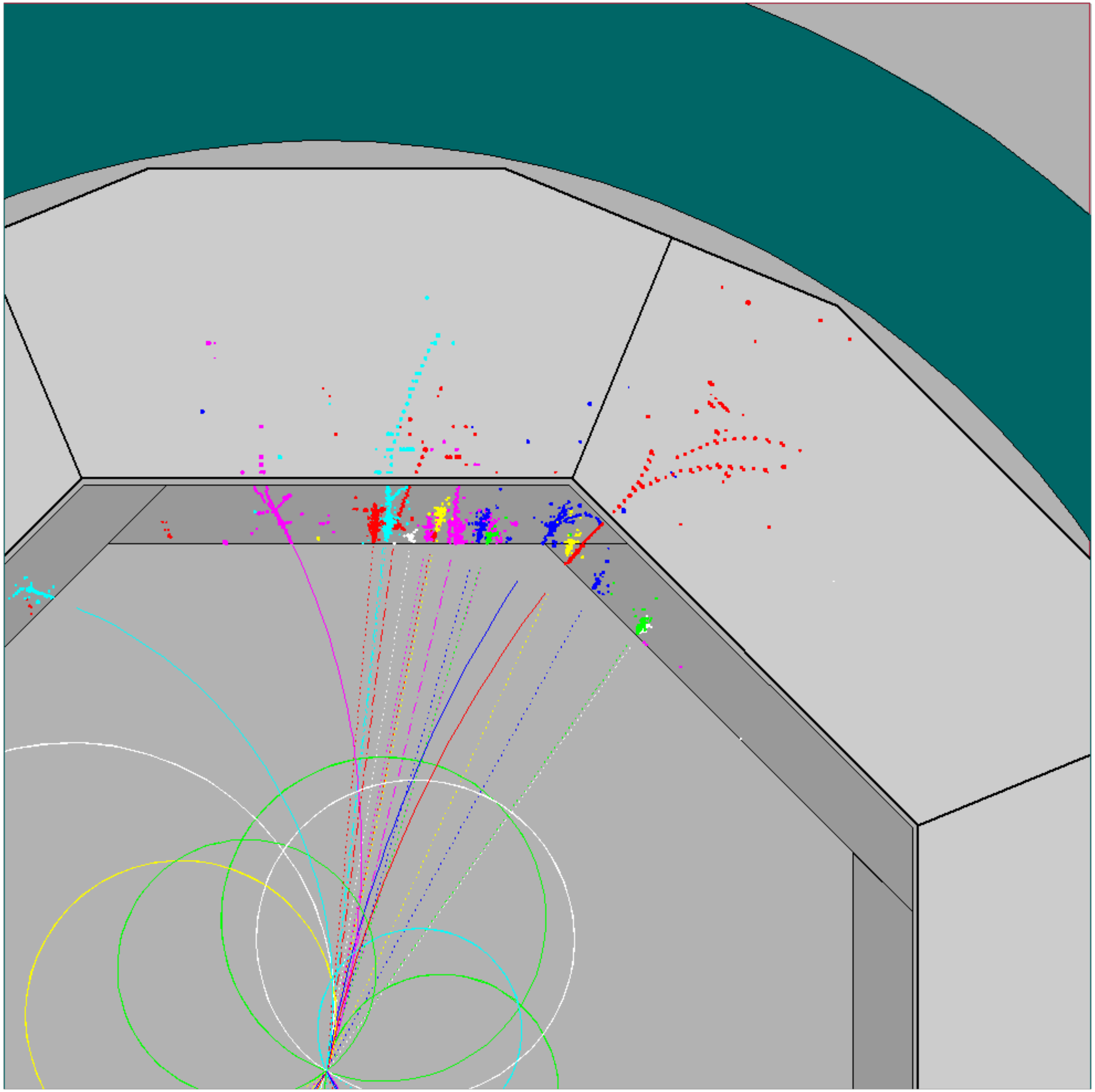

The hadron calorimeter

Jet energy: $\frac{\sigma_E}{E} \simeq 0.30 \frac{1}{\sqrt{E(\mathrm{GeV})}}$

(1/200 calorimeter granularity w.r.t. LHC)

e.g: Separation of WW and ZZ

$$e^+e^- \rightarrow \nu\bar{\nu}W^+W^-, \nu\bar{\nu}ZZ\,, \quad W, Z \rightarrow 2\mathrm{jets}$$

$$\frac{\sigma_E}{E} = \frac{0.6}{\sqrt{E}}$$

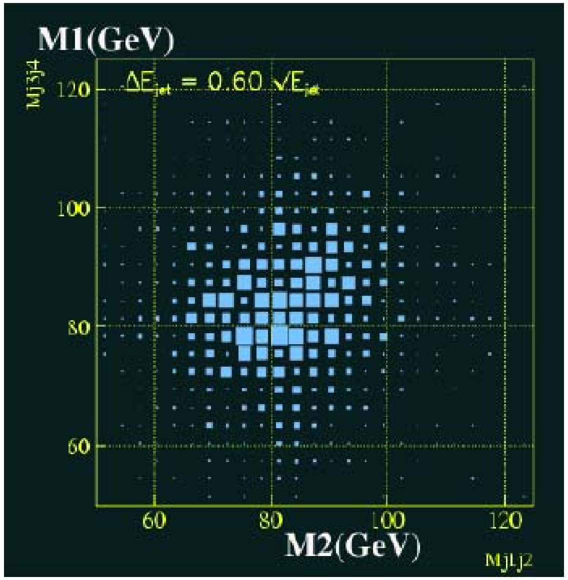

$$\frac{\sigma_E}{E} = \frac{0.3}{\sqrt{E}}$$

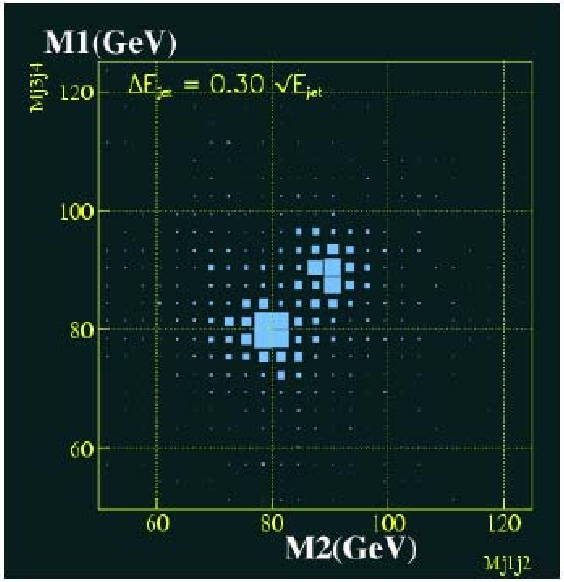

Granularity is essential
('Imaging calorimeter')
On/off read-out
Digital HCAL?

$\frac{\sigma_E}{E} \sim \frac{0.3}{\sqrt{E}}$ is 'needed'.

The Hadron Calorimeter

Tile-fibre calorimeter

Centre/straight WLS-fibre

Diagonal/bent WLS-fibre

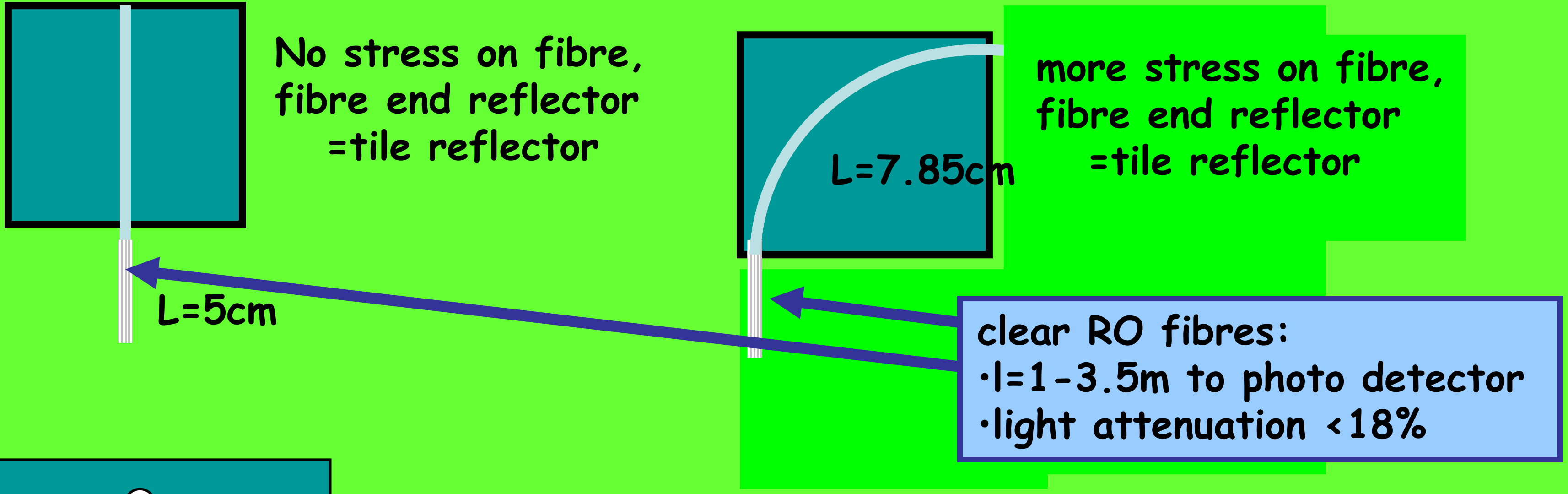

No stress on fibre,
fibre end reflector
=tile reflector

more stress on fibre,
fibre end reflector
=tile reflector

clear RO fibres:
- l=1-3.5m to photo detector
- light attenuation <18%

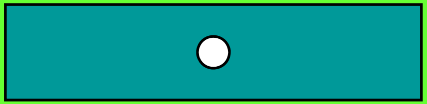

1.4 mm hole in centre
- drilled and polished
- For 5 cm straight WLS-fibre RO
- cheep, for SiPM's only

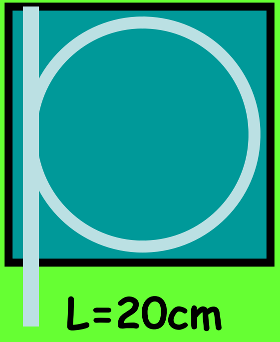

Single looped fibre
- strong fibre bending,
- most stress on fibres,
- probably ageing damages?

Light yield for MIP's (used for calibration): 18-25 ph.e. on photo-cathode

β -source with 1 mm collimator

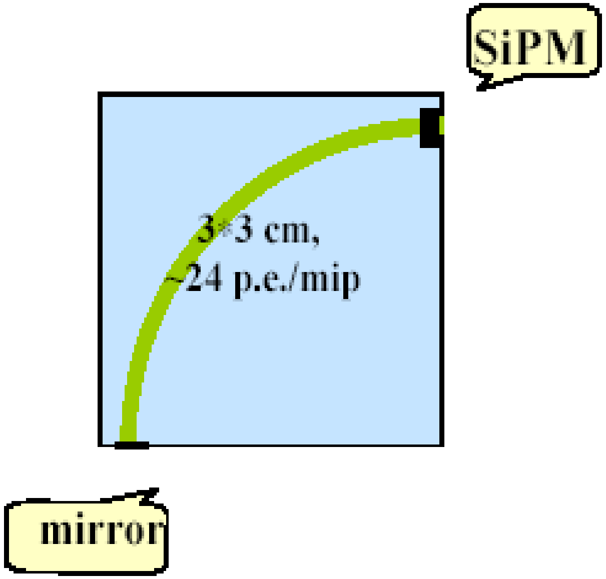

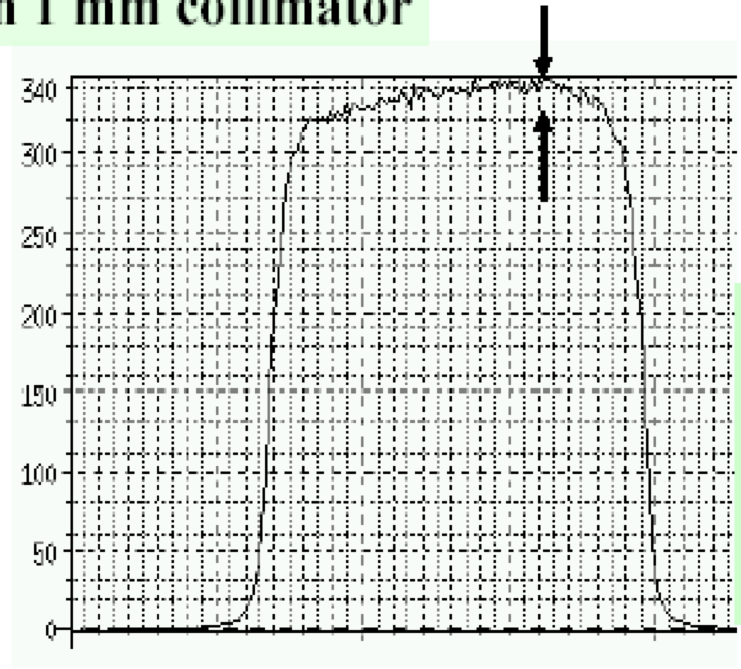

Max amplitude variance ~5% for scanning along the median line (3 * 3 cm² tile)

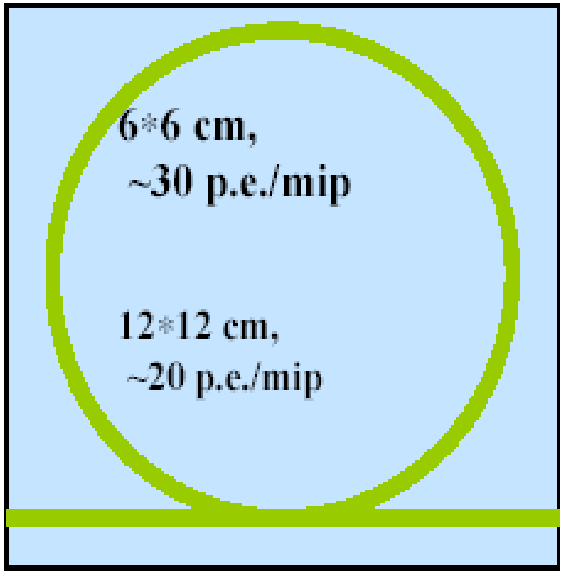

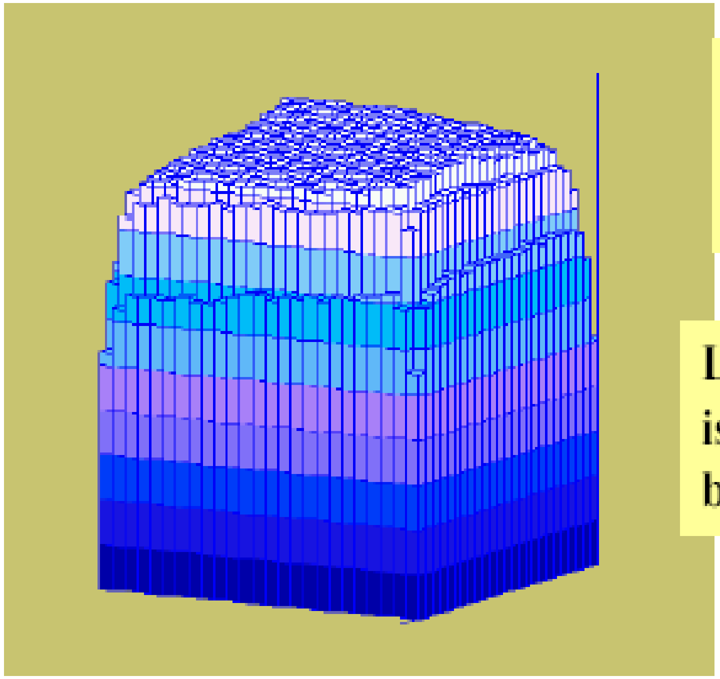

Scanning with β -source over 6 * 6 cm² tile

Light Yield uniformity is ~ 3% except of boundaries

Test of 3 types of Photo-Detector

MA-PM -16 channels (Hamamatzu):
- best photo-detector
- cannot be operated in magnetic field
- single tile or cell read out

Only for reference

Silicon photo-multiplier (SiPM):
- new detector concept, first test with beam
- sizes: 1x1mm², 1024 pixels/mm²
- gain ~ 1*10⁶ ➔ No preamplifier needed
- quantum eff. ~ 15-20%
- single tile read out / mounted directly on tile

Silicon PhotoMultiplier (SiPM)
MEPhI&PULSAR

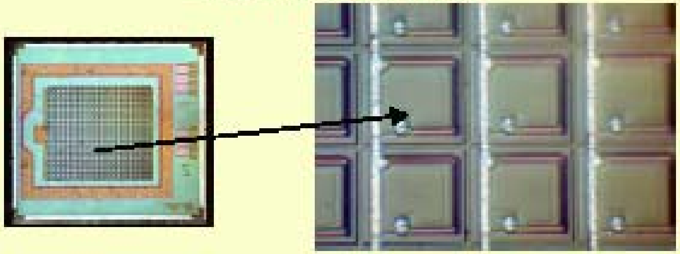

SiPM

Pixels of the SiPM

Avalanche photo-diode (APD,Hamamatzu S8664-55spl):
- different from those used by CERN experiments
- 3x3mm² low capacity
- gain ~ 200 ➔various preamp board tested @ DESY
- quantum eff. ~ 75%
- cell read out: 3 tiles

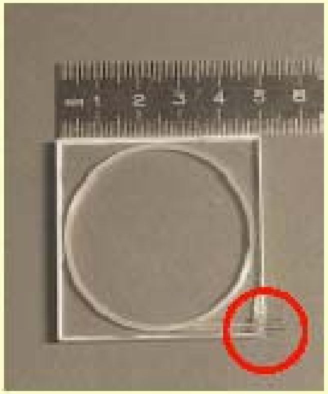

Fragment of Scintillator - WLS - SiPM readout cell

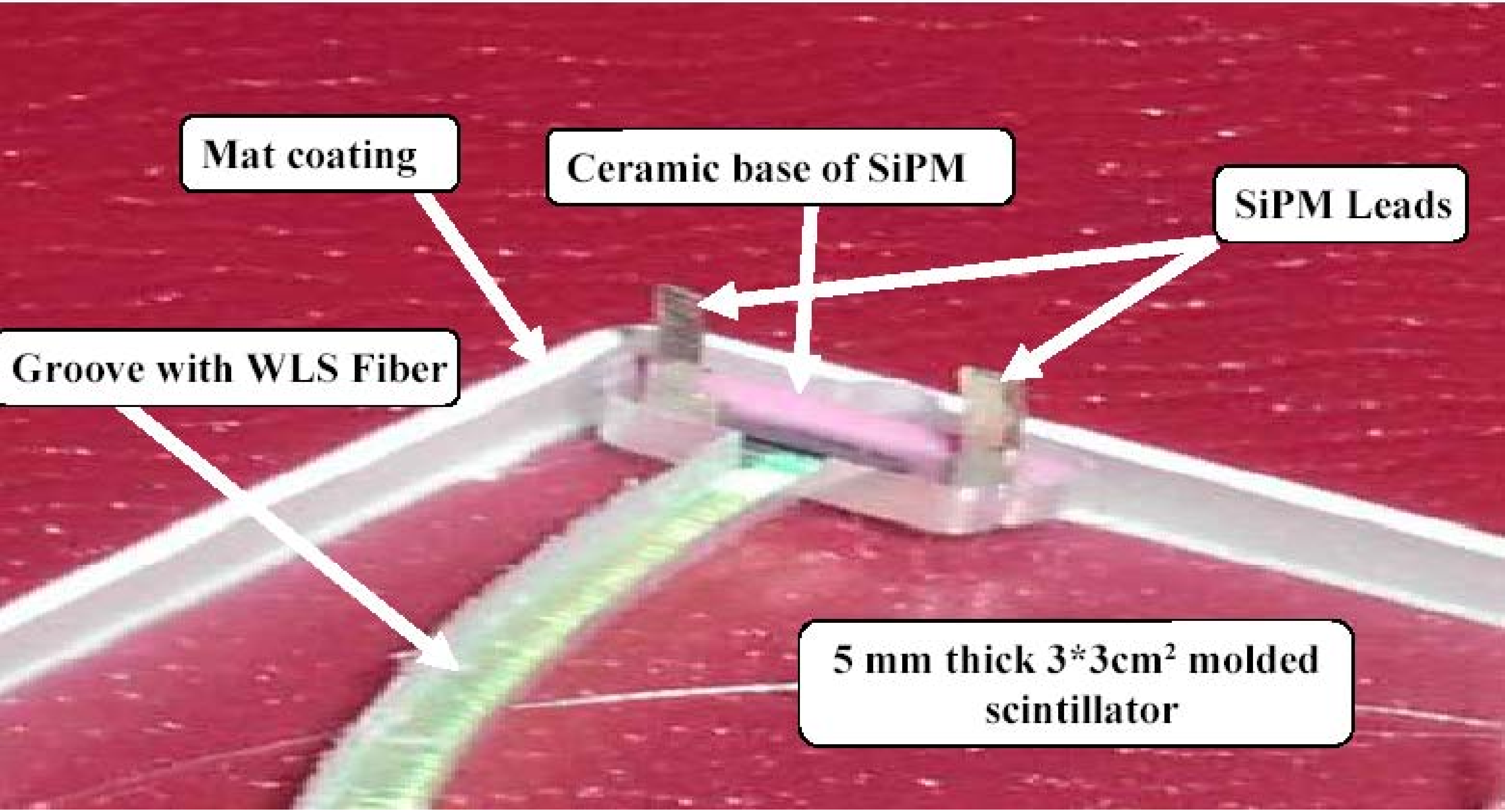

Mat coating

Ceramic base of SiPM

SiPM Leads

Groove with WLS Fiber

5 mm thick 3*3cm² molded scintillator

MIP Calibration

➔ Obtained using 3 GeV electron beam on single tile, w/o absorber in front

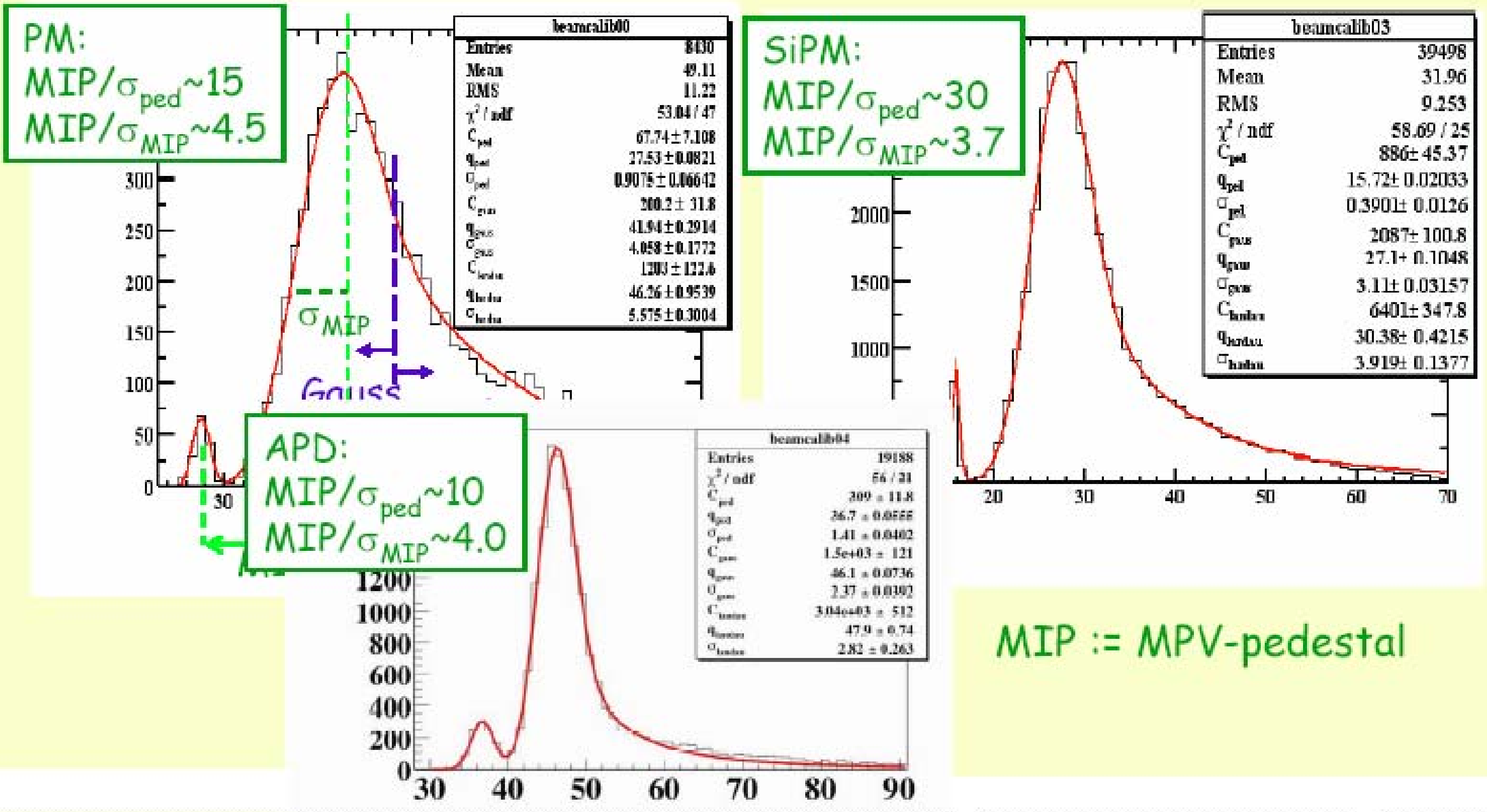

PM:
MIP/σ_{ped}~15
MIP/σ_{MIP}~4.5

SiPM:
MIP/σ_{ped}~30
MIP/σ_{MIP}~3.7

APD:
MIP/σ_{ped}~10
MIP/σ_{MIP}~4.0

MIP := MPV-pedestal

Energy Resolution

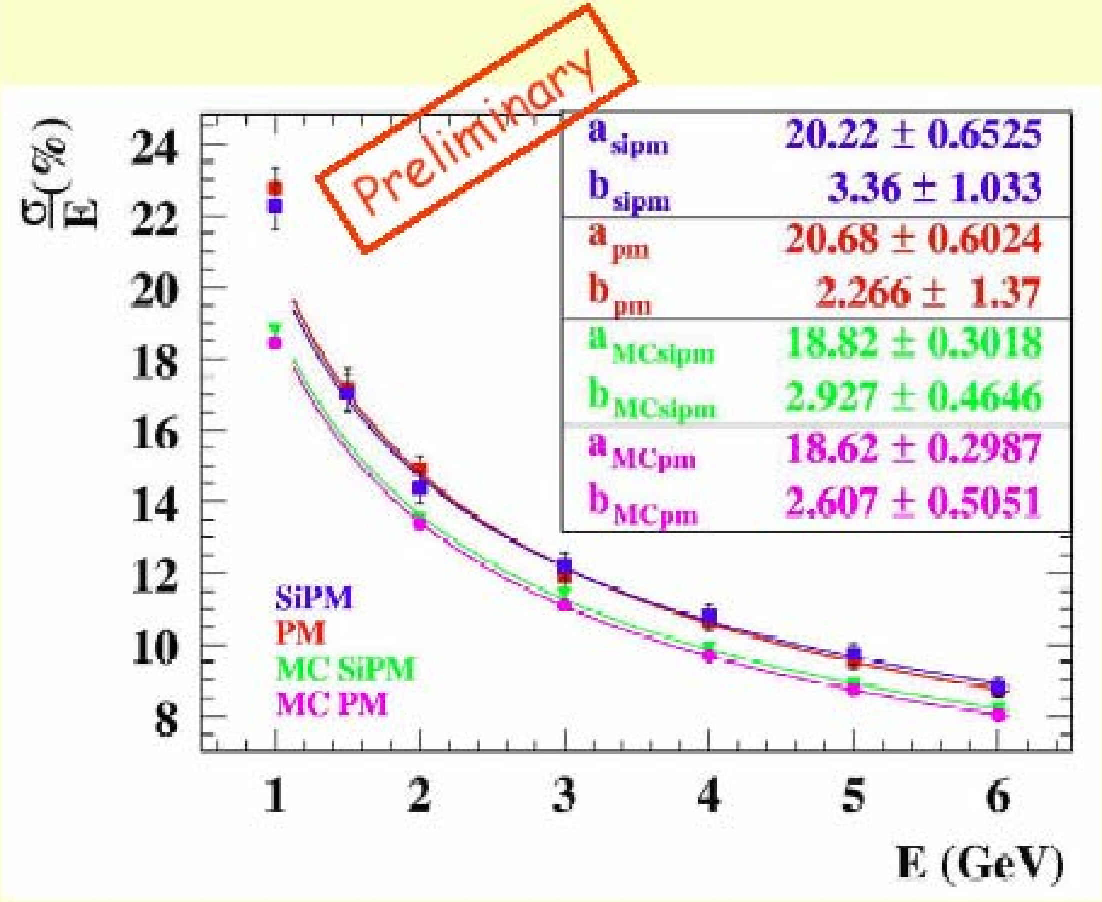

➔Very good agreement between PM and SiPM on the whole range 1 - 6 GeV

➔Low sensitivity to constant term due to limited energy range

➔MC tuning still in progress include more effects:
-beam energy spread
-steal thickness tolerances

The digital hadron calorimeter

Very high granularity (~1cm^2) with 1-bit read-out

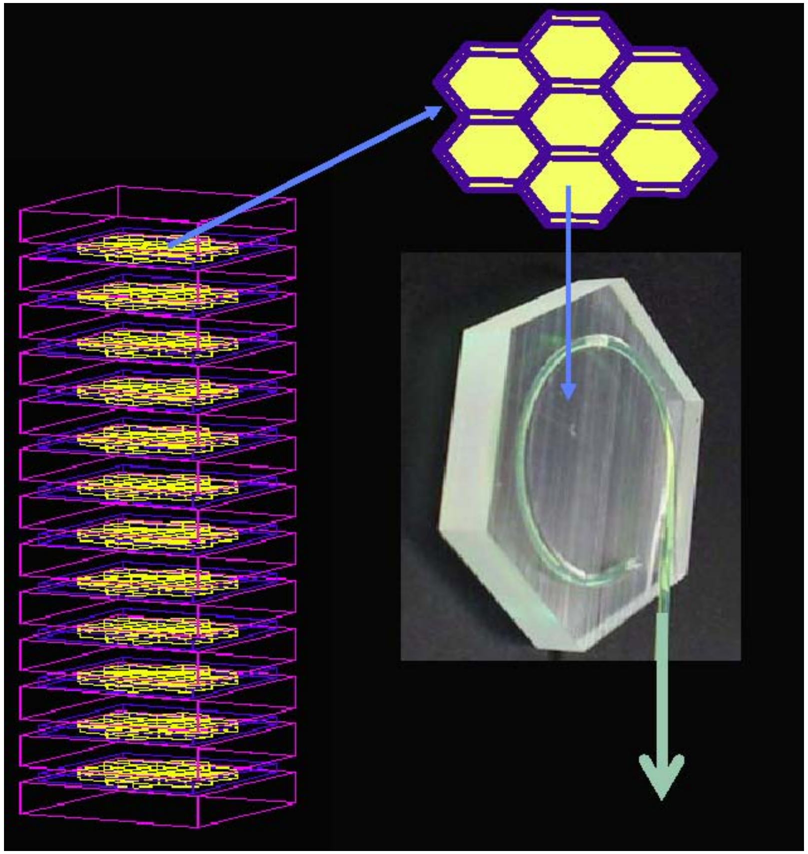

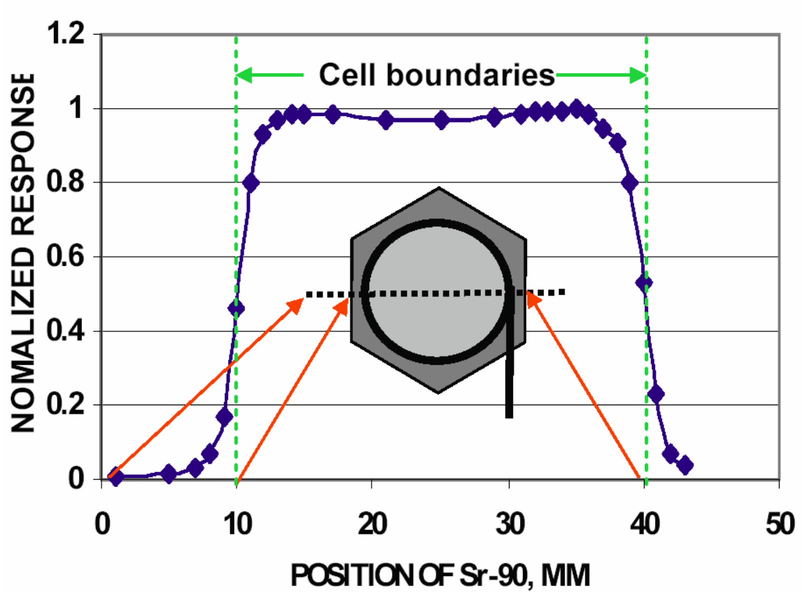

Uniformity within cell 3%

Analogue/digital response for hadrons

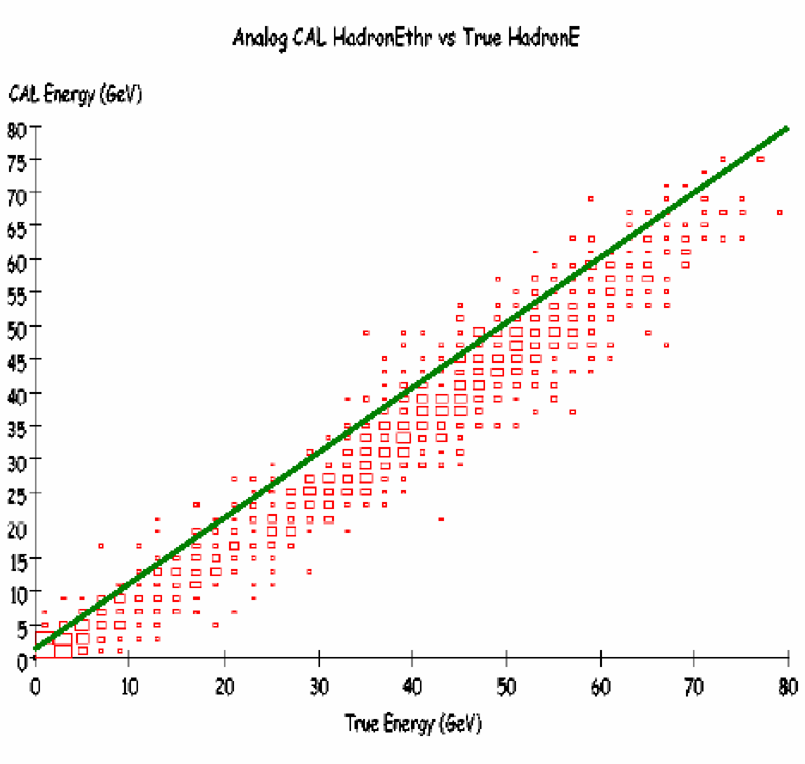

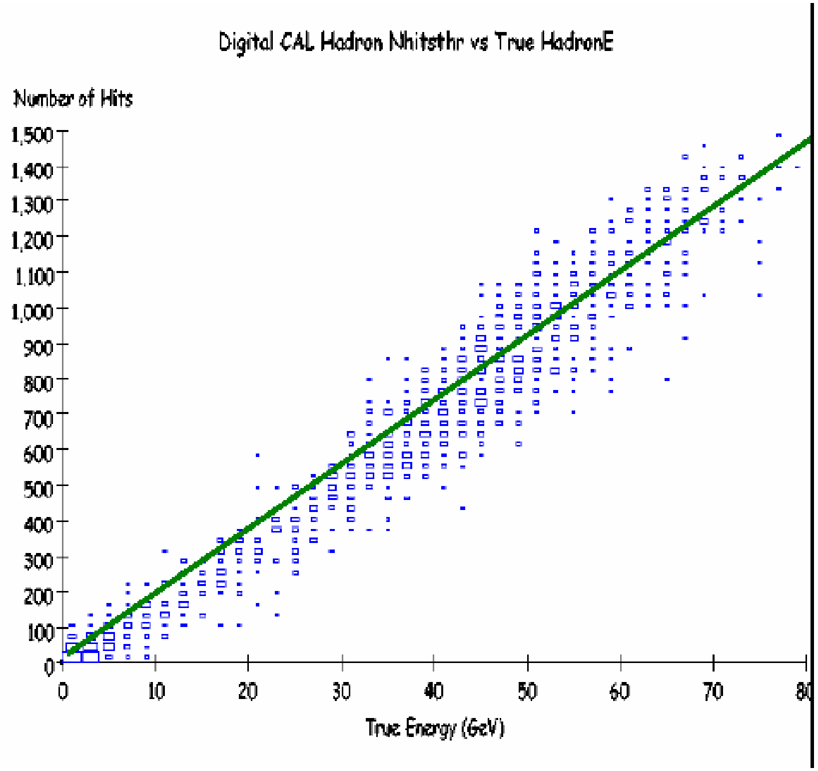

Analogue calorimeter sum energy whereas digital calorimeter sum hits

Digital calorimeter: sampling fluctuations are fluctuations in the total number of tracks crossing the sensitive planes.

Analog vs Digital Energy Resolution

GEANT 4 Simulation of SD Detector (5 GeV π^+)

-> sum of ECAL and HCAL analog signals - Analog

-> number of hits with 10 MeV threshold in HCAL - Digital

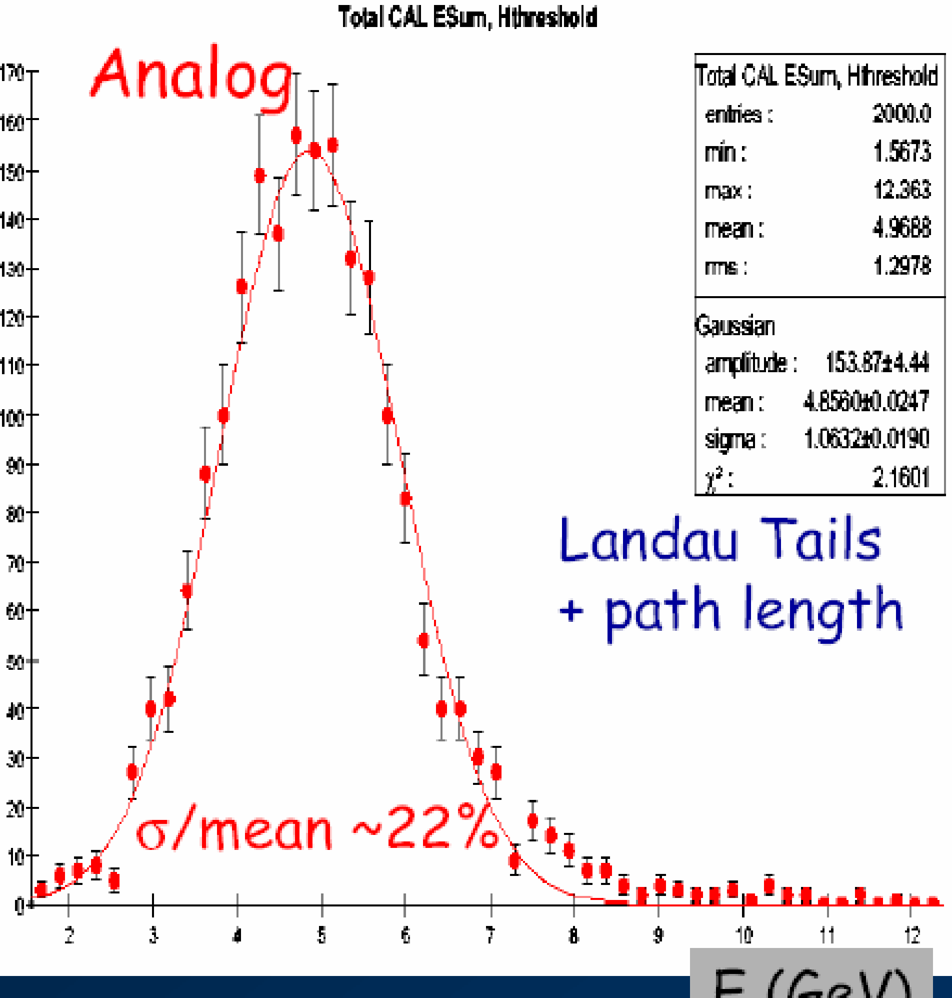

Analog

Landau Tails + path length

σ/mean ~22%

E (GeV)

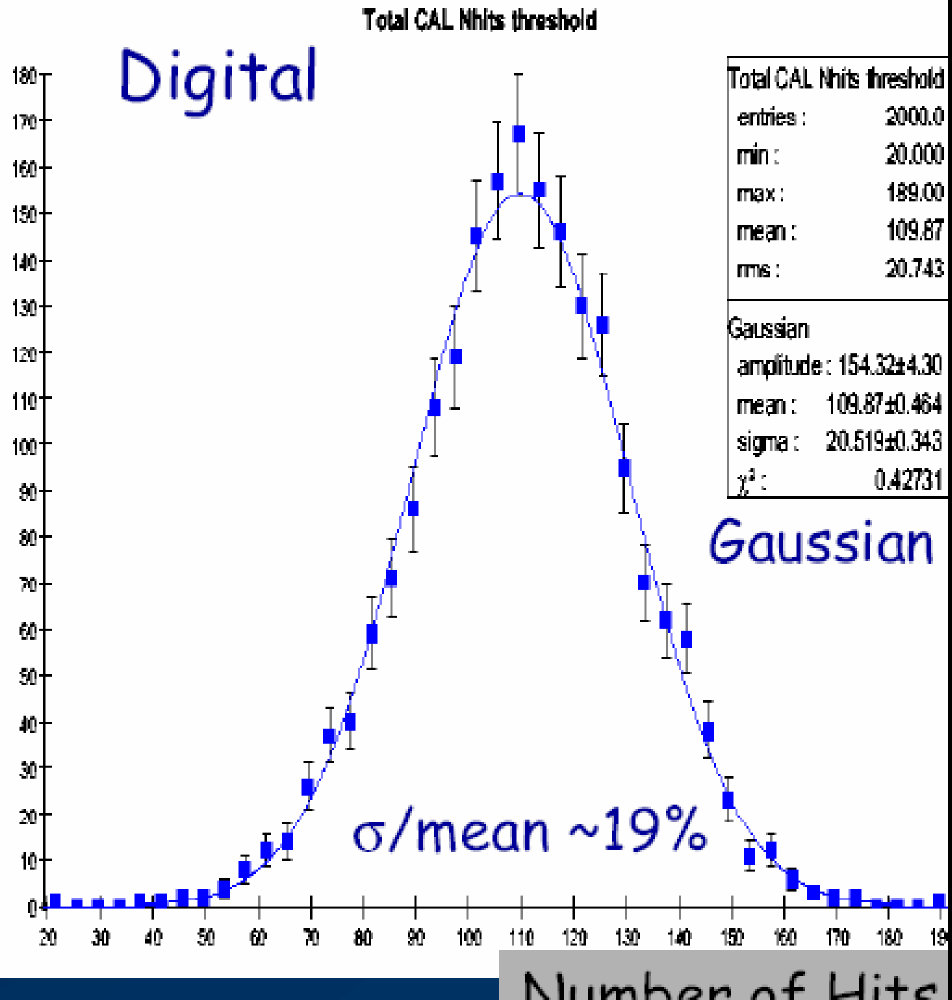

Digital

Gaussian

σ/mean ~19%

Number of Hits

Summary

- The physics programme of both the LHC and the ILC will be very rich
- The high energy of the LHC leads to a large mass reach for the discovery of heavy new particles
- The clean experimental environment of the ILC allows detailed studies of directly acceptible new particle and gives rise to a high sensitivity to indirect effects of new physics.
- The physics at LHC and ILC is complementary in many respects

Why Super Conducting RF?

- Low RF losses in resonator walls
  ($Q_0 \approx 10^{10}$ compared to Cu $\approx 10^4$)
  - high efficiency $\eta_{AC \rightarrow beam}$
  - long beam pulses (many bunches) → low RF peak power
  - large bunch spacing allowing feedback correction within bunch train.
- Low-frequency accelerating structures
  (1.3 GHz, for Cu 6-30 GHz)
  - very small *wakefields*
  - relaxed alignment tolerances
  - high beam stability

The positron source

Thin single target
Undulator based
Location in linac
Impact on operation

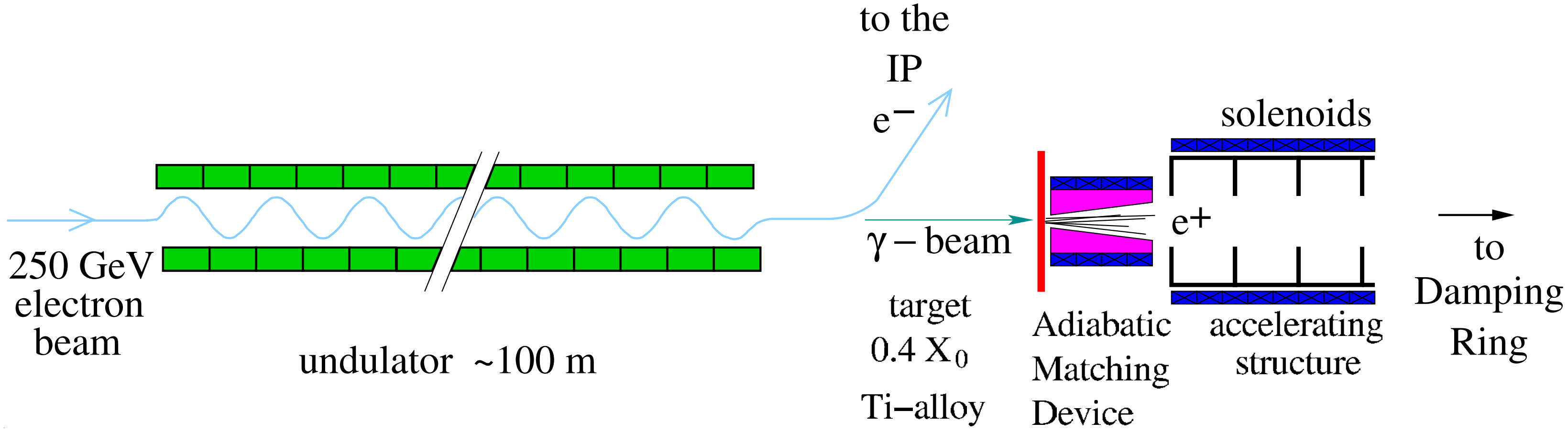

ILC Projected Time Line